REPORT No. 317

WIND TUNNEL TESTS ON A SERIES OF WING MODELS THROUGH A LARGE ANGLE OF ATTACK RANGE PART I—FORCE TESTS

By MONTGOMERY KNIGHT and CARL J. WENZINGER
Langley Memorial Aeronautical Laboratory

REPORT No. 317

WIND TUNNEL TESTS ON A SERIES OF WING MODELS THROUGH A LARGE ANGLE OF ATTACK RANGE

PART I. FORCE TESTS

By Montgomery Knight and Carl J. Wenzinger

SUMMARY

This investigation covers force tests through a large range of angle of attack on a series of monoplane and biplane wing models. The tests were conducted in the atmospheric wind tunnel of the National Advisory Committee for Aeronautics. The models were arranged in such a manner as to make possible a determination of the effects of variations in tip shape, aspect ratio, flap setting, stagger, gap, decalage, sweep back, and airfoil profile. The arrangements represented most of the types of wing systems in use on modern airplanes.

The effect of each variable is illustrated by means of groups of curves. In addition, there are included approximate autorotational characteristics in the form of calculated ranges of "rotary instability."

A correction for blocking in this tunnel which applies to monoplanes at large angles of attack has been developed, and is given in an appendix.

INTRODUCTION

The need of greater safety in airplane flight leads to a consideration of the characteristics of wing systems at low speeds or large angles of attack. In general, the region of danger lies above the angle of maximum lift, and comparatively little information has been published relating to the landing, spinning, stability, and controllability of airplanes in this region.

In order to augment the information on this subject, a comprehensive test program is being carried out in the atmospheric wind tunnel at the Langley Memorial Aeronautical Laboratory. This program includes force, pressure distribution, and autorotation tests on a series of models representing most of the wing systems in use on modern airplanes. The angle of attack range of the tests is sufficiently large to cover practically all attitudes attainable by an airplane in flight.

The force test part of the program has been completed, and the results have already been published in part. (Reference 1.) The present report gives the complete information as to lift, drag, and resultant force, and also includes the calculated probable ranges of "rotary instability," an important phase of autorotation. With reference to rotation about a fixed axis in the plane of symmetry, and parallel to the wind direction, certain terms relating to autorotation are of importance, and may be defined as follows:

1. "Rotary instability" signifies a state of equilibrium in rectilinear motion such that rotations caused by small disturbances will increase in rate until a uniform angular velocity has been attained.

2. "Rotary stability" signifies a state of equilibrium in rectilinear motion such that rotations caused by small disturbances will decrease in rate until the angular velocity becomes zero.

3. "Neutral rotary equilibrium" signifies that state of equilibrium existing between the conditions of rotary stability and instability.

MODELS AND TESTS

The wing models which were constructed of laminated mahogany had a 5-inch chord and an aspect ratio of 6, except as noted in Tables I and II. The Clark Y profile was employed in all but a few of the tests in which the N. A. C. A. M-1 profile was used. With the exception of those tested to show tip effects, circular tipped models were used throughout.

The upper and lower wings of the biplane models were connected by means of two streamlined struts spaced 0.6 chord length apart, located along the span, 0.45 chord length from the leading edge and equidistant from the midspan. These struts fitted into sockets built into the wings. The sockets were designed so that the struts could be inclined in a fore and aft direction, and clamped rigidly in position. This arrangement, used in combination with struts of different lengths, made it possible to vary gap, stagger, and decalage as desired.

All of the force tests were conducted in the 5-foot atmospheric wind tunnel (Reference 2), which has a circular, closed-throat test section. The models were mounted in the wind tunnel on the usual wire balance as shown in Figure 1.

The tests were arranged to enable the determination of the effects produced by the variations in the wing models shown in Tables I and II. Lift, drag, and pitching moment were

FIGURE 1.—Biplane set up in wind tunnel

measured for angles of attack ranging from $-45°$ to $+90°$. Due to the nature of the set-up, it was necessary for the complete test on each model to be made in three parts, the angle of attack range of one part overlapping by a few degrees that of the next.

The tests were conducted at an average dynamic pressure of 19.93 kg. per m^2 corresponding to an average air speed of 17.9 meters per second (40.0 M. P. H.), and an average Reynolds Number of 153,000.

All drag readings were corrected for the drag of the supporting system. The biplane strut drag was found to be negligible, and was therefore disregarded.

The test results are not corrected for tunnel wall interference for the following reasons:

a. The Prandtl correction for tunnel wall interference effects on the wing-tip vortices is known to be accurate only up to maximum lift. In general, it appears that at about 25° angle of attack this correction becomes negligible. However, between the angle of maximum lift and 25° the amount of the correction is not known, and in consequence it has been omitted.

b. At approximately 25° the blocking of the air flow by the model causes an increase in effective dynamic pressure in the region of the model. This effect reaches a maximum at an

TABLE I

MONOPLANE WING TESTS

Variable	Tip	Aspect ratio	Flap	Profile	Figure No.
Tip	Rectangular	6	0	Clark Y	2, 3, 4, 5, 6, 7.
	Negative rake	6	0	do	
	Circular	6	0	do	
Aspect ratio	do	4	0	do	7, 8, 9, 10, 11, 12.
	do	6	0	do	
	do	8	0	do	
Flap (20 per cent chord)	do	6	15° up	do	7, 13, 14, 15, 16, 17, 18, 19.
	do	6	0°	do	
	do	6	15° down	do	
	do	6	25° down	do	
	do	6	30° down	do	
Profile	do	6	0	do	7, 20, 21, 22, 23.
	do	6	0	N. A. C. A.-M1	

TABLE II

BIPLANE WING TESTS

Variable	Stagger	Gap/chord	Decalage	10° Sweep back		Profile		Figure No.
				Upper wing	Lower wing	Upper wing	Lower wing	
	Per cent		*Degrees*					
Stagger	−25	1.0	0	0	0	Clark Y	Clark Y	24, 25, 26, 27, 28, 29, 30.
	0	1.0	0	0	0	do	do	
	+25	1.0	0	0	0	do	do	
	+50	1.0	0	0	0	do	do	
Gap	0	1.5	0	0	0	do	do	28, 31, 32, 33, 34, 35.
	0	1.0	0	0	0	do	do	
	0	0.5	0	0	0	do	do	
Decalage	0	1.0	+3	0	0	do	do	28, 36, 37, 38, 39, 40.
	0	1.0	0	0	0	do	do	
	0	1.0	−3	0	0	do	do	
Sweep back [1]	0	1.0	0	Straight	Sweep back	do	do	41, 42, 43, 44, 45, 46, 47.
	0	1.0	0	Sweep back	Straight	do	do	
	+50	1.0	0	do	do	do	do	
	−50	1.0	0	Straight	Sweep back	do	do	
Profile	0	1.0	0	0	0	do	do	28, 48, 49, 50, 51, 52.
	0	1.0	0	0	0	do	N. A. C. A.-M1	
	0	1.0	0	0	0	N. A. C. A.-M1	Clark Y	

[1] Stagger measured at midspan.

angle of attack of about 90° for a given wing. Tests have been made from which a correction for blocking has been derived, and the results are given in the appendix. This correction, however, applies to monoplanes only, and hence it has not been used in this report, which covers biplanes as well as monoplanes. The determination of the blocking corrections for biplane wings is a problem which requires further research.

The lift, drag, and pitching moment were measured in general to within an accuracy of ± 1.5 per cent. In the construction of the wing models the tolerance with reference to the airfoil ordinates was ± 0.003 inch.

RESULTS

For purposes of direct comparison, the test results are presented in groups of curves and diagrams, each group showing the effects of one of the variables as listed in Tables I and II. These groups, given in Figures 2 to 52, are arranged for each variable in four consecutive sections as follows:

(a) Absolute lift and drag coefficients vs. angle of attack (C_L and C_D vs. α).
(b) Polars (C_L vs. C_D).
(c) Center of pressure coefficients vs. angle of attack (C_p vs. α).
(d) Vector diagrams.

In the center of pressure curves for the monoplanes, the plotted points represent the intersection of the resultant force vectors with the wing chord line. Similarly, the "mean chord" (halfway between the chords of the upper and lower wings as indicated on the vector diagrams) of the biplane models was used in obtaining the C_p values. It should be borne in mind that the C_p curves illustrated hold good only for the base lines assumed, and that any other reference lines would give different results.

Lift and drag coefficients and angle of attack for each complete force test are given in Tables IV to XXVII, inclusive.

The calculated probable ranges of "rotary instability" for each model tested are indicated in Table III. These ranges were obtained by noting the points on the polar curves at which radial lines through the origin were perpendicular to the curves. Each point of intersection signifies a state of "neutral rotary equilibrium," as previously defined, and is shown as such on the comparative polar curve groups. Then where the slope of the curve is negative between these points with respect to the radial lines, the wing model will be capable of autorotation, i. e., will be in a state of "rotary instability." The negative slope indicates a decreasing resultant force with increasing angle of attack, and this is the criterion for "rotary instability," which may be expressed as—

$$\frac{d\,(C_R)}{d\,\alpha} < 0$$

(See Reference 3 for derivation), where C_R is the absolute coefficient of resultant force, and α is the angle of attack of the wing. This criterion, however, is an approximation, subject to the limitations of the "strip method" of autorotation calculation, which assumes a uniform distribution of the resultant force along the span, for the wing in rectilinear motion.

DISCUSSION OF RESULTS

A general survey of the curves and diagrams demonstrates the appreciable effects which changes in the geometry of wing systems have on lift, drag, and center of pressure, particularly at large angles of attack. It will be noted that the effect on drag is the most marked, and the influence of stagger is greater than that of gap or decalage. The effects of variations in stagger, gap, and sweep back, at the large angles of attack, are largely due to the partial shielding of the biplane upper wing by the lower. (Reference 4.)

Referring now to the curves in greater detail, the effects of the variables on the aerodynamic characteristics of the wing models may be listed as follows:

MONOPLANES

1. TIPS

LIFT (figs. 2, 3):

Maximum C_L is highest for rectangular tips, next for negative raked tips, and lowest for the circular tips, although the difference is small.

DRAG (figs. 2, 3):

Minimum C_D shows little difference, and in general C_D is much the same for the three models with different tip shapes.

CENTER OF PRESSURE (figs. 4, 5, 6, 7):

The C_p curves show little variation for the three different tips, and the differences may be explained as due to the different dispositions of the wing area.

2. ASPECT RATIO

LIFT (figs. 8, 9):

Maximum C_L increases with increase of aspect ratio. The slope of the lift curve below maximum C_L becomes greater due to the decrease in the induced angle of attack. This decrease is also partly due to tunnel wall interference.

DRAG (figs. 8, 9):

Minimum C_D is practically the same for the aspect ratios investigated. The effects of aspect ratio and the tunnel walls on induced drag are apparent below maximum lift. Above 20° angle of attack, C_D increases in the order of the aspect ratio and the differences are due in great measure to blocking effects at large angles.

CENTER OF PRESSURE (figs. 7, 10, 11, 12):

The C_p curves for the different aspect ratios covered in the tests are practically the same.

3. FLAP

LIFT (figs. 13, 14):

Maximum C_L increases with increasing flap angle in the downward direction, and occurs at slightly lower angles of attack. Moving the flap downward through a given angle increases the lift by an amount approximately equal to the decrease produced by moving it up through the same angle. It will be noted that in Figure 13, just beyond each of the primary and secondary lift peaks the changes in lift are small.

DRAG (figs. 13, 14):

Above zero angle of attack the drag increases in a regular manner, both with increasing angle of attack and with flap moving from up to down postions.

CENTER OF PRESSURE (figs. 7, 15, 16, 17, 18, 19):

For angles of attack above zero lift the *C. P.* travel becomes smaller with decreasing flap angle, due to the decrease of the effective camber of the wing. With the flap displaced upward 15°, the travel is backward above zero lift. For flap settings of from 15° to 30° down, the C_p curves are much the same above zero lift, but are displaced to the rear with respect to the neutral flap curve. Attention is called to the marked difference in the shape of the curves for the 15° upward and downward flap displacements below zero lift.

4. PROFILE

LIFT (figs. 20, 21):

Maximum C_L is much higher for the Clark Y than for the symmetrical N. A. C. A.–M1. The angle of zero lift is higher for the N. A. C. A.–M1, due to its straight mean camber line.

DRAG (figs. 20, 21):

From −3° to +8°, the drag of the N. A. C. A.–M1 is less than that for the Clark Y, and is greater from +8° to 18°. Above 18°, and below −3°, C_D for the N. A. C. A.–M1 is the lower.

CENTER OF PRESSURE (figs. 7, 22, 23):

The *C. P.* travel for the N. A. C. A.-M1 is practically negligible from $-6°$ to $+6°$ angle of attack, and then moves rearward. The Clark Y, however, has a forward motion of *C. P.* up to 12° angle of attack, and rearward beyond this angle.

BIPLANES

5. STAGGER

LIFT (figs. 24, 25):

Maximum C_L increases with increase of stagger up to +25 per cent and then remains the same for 50 per cent stagger, although occurring at a slightly smaller angle of attack.

DRAG (figs. 24, 25):

Minimum C_D is highest for the zero stagger. Above the angle of maximum C_L, however, C_D increases greatly with increase in stagger. These effects on drag at the large angles of attack are due mainly to the partial shielding of the upper wing of the biplanes by the lower.

CENTER OF PRESSURE (figs. 26, 27, 28, 29, 30):

The distance traveled back by the *C. P.* above maximum C_L becomes greater with increasing stagger. The peculiar behavior of negative stagger at large angles of attack should be noted.

6. GAP

LIFT (figs. 31, 32):

Maximum C_L increases up to G/c ratio of 1.0 where it appears to remain constant for G/c ratio increase, although the slope of the lift curve becomes greater with higher G/c ratios. This is due to the decrease in induced angle of attack with increasing gap.

DRAG (figs. 31, 32):

Minimum C_D is approximately the same for the G/c ratios tested. For the large angles of attack, C_D increases with increasing G/c ratios.

CENTER OF PRESSURE (figs. 28, 33, 34, 35):

As the G/c ratio is increased, the *C. P.* above maximum lift recedes farther with increase of angle of attack up to 50°, although not as far as for the staggered biplanes.

7. DECALAGE

LIFT (figs. 36, 37):

Positive and negative decalage cause a lower maximum C_L than zero decalage, but the magnitude is about the same for the same values of decalage, plus or minus. For positive decalage, maximum C_L occurs at a smaller angle of attack, and that of negative decalage at a larger angle than that for zero decalage.

It can also be seen that the lift and drag curves for positive or negative decalage are shifted by an approximately constant angle to one or the other side of those for zero decalage. Since the lower wing of the biplane was set at $\pm 3°$ with respect to the upper wing at zero lift, the "effective" angle of attack becomes respectively 1.5° minus or plus the angle of attack of zero lift for no decalage.

DRAG (figs. 36, 37):

Maximum C_D shows little difference for the angles of decalage investigated, but C_D increases with increase of decalage.

CENTER OF PRESSURE (figs. 28, 38, 39, 40):

Negative decalage causes a more rapid recession of the *C. P.* above maximum C_L, with increase of angle of attack, than does either zero or positive decalage. The sharp peak on the $-3°$ curve is remarkable.

The effects of decalage are not as great as those produced by stagger, but they are greater than those due to changes in gap.

8. SWEEP BACK

LIFT (figs. 41, 42):

Maximum C_L occurs at about the same angle of attack for all conditions tested. C_L is highest for +50 per cent stagger at midspan with the upper wing swept back, and lowest for the same combination with zero stagger.

The similarity is very striking between the lift curves of the two combinations with upper wing swept back, +50 per cent midspan stagger, and lower wing swept back, zero stagger. The other two combinations tested are also very similar, and this indicates that sweep back in one wing is, effectively, stagger. No appreciable difference is shown whether the stagger used with the swept-back wing is at the tips or at midspan.

DRAG (figs. 41, 42):

The similarity between the drag curves of the same pairs of combinations as noted in the case of lift, is very noticeable, and also indicates that sweep back in one wing is, in effect, stagger.

CENTER OF PRESSURE (figs. 43, 44, 45, 46, 47):

The most noticeable effect brought out by the C_p curves is the fairly close resemblance between the results for the biplane with upper wing swept back, zero midspan stagger, and that with the lower wing swept back, −50 per cent midspan stagger.

9. PROFILE

LIFT (figs. 49, 50):

The N. A. C. A.–M 1 in combination with the Clark Y gives a lower maximum C_L than with both wings Clark Y, and the lift curves have more rounded peaks.

DRAG (figs. 49, 50):

Minimum C_D is slightly lower for the combination of N. A. C. A.–M1 wing lower and Clark Y upper. In general, with both wings Clark Y, the drag is slightly higher at large angles of attack.

CENTER OF PRESSURE (figs. 28, 48, 51, 52):

The C_p curves for the three combinations tested do not show any great variations. The combination of the N. A. C. A.–M1 lower wing and Clark Y upper wing is probably the most desirable from the standpoint of safety, due to the smaller slope of the curve in the region of the angle of maximum C_L, which means less instability longitudinally.

10. ROTARY INSTABILITY

From a consideration of the calculated ranges of rotary instability (Table III), the following points may be noted:

None of the monoplanes show any tendency toward autorotation above 26°, but the biplanes indicate additional autorotational tendencies above this angle.

Positive stagger is seen to reduce the tendency of the biplanes to autorotate at the large angles, while increase in gap within practical limits has a similar effect, only to a smaller degree

Sweep back arranged so as to give positive stagger at the tips appears to reduce the range of rotary instability at large angles of attack. Geometrically, sweep back in one wing of a biplane is merely a progressive change in stagger along the span. The criterion for rotary instability is based on the assumption of uniform span loading, and for this reason the points of neutral rotary equilibrium are only roughly approximate for the swept-back wing combinations.

Decalage seems to have no appreciable effect in reducing the rotary instability ranges of the biplanes.

CONCLUSIONS

Since these force tests have been made at the low Reynolds Number of 153,000, any conclusions as to the effects of the variable factors should be drawn with that in mind. As the effects at angles of attack below maximum lift have already been fully investigated, the conclusions given here apply to the results at maximum C_L and above.

MONOPLANES

1. Tips.—Different shaped tips produce only small effects.

2. Aspect ratio.—Increase of aspect ratio slightly increases maximum C_L, and C_D also increases at large angles.

3. Flap.—Moving the flap down increases maximum C_L which occurs at slightly lower angles of attack. C_D also increases with downward movement of the flap.

4. Profile.—The Clark Y has a much higher maximum C_L than the N. A. C. A.-M1.

BIPLANES

5. Stagger.—Increase in stagger raises the maximum C_L, and greatly increases C_D above the angle of maximum lift.

6. Gap.—Larger gap slightly increases the maximum C_L, and causes an increase in C_D, although the effects are not as great as those of stagger.

7. Decalage.—Positive and negative decalage have very little effect except to shift the lift and drag curves as a whole to one side or the other of those for zero decalage.

8. Sweep Back.—Sweep back may be considered as a form of stagger, since the result of combining a swept-back wing with a straight wing in a biplane is similar to staggering a straight wing biplane.

9. Profile.—The N. A. C. A.-M1 wing in combination with the Clark Y gives lower maximum C_L than with both wings Clark Y, and the lift curve peaks are more rounded.

10. Rotary Instability.—The autorotational characteristics of wing systems are greatly affected by changes in profile and in the geometrical arrangement of the wings.

BIBLIOGRAPHY

Reference 1

Wenzinger, C. J., and Harris, T. A.: Wind Tunnel Force Tests on Wing Systems through Large Angles of Attack. N. A. C. A. Technical Note No. 294 (1928).

Reference 2.

Reid, Elliott G.: Standardization Tests of N. A. C. A. No. 1 Wind Tunnel. N. A. C. A. Technical Report No 195 (1924.)

Reference 3.

Knight Montgomery: Wind Tunnel Tests on Autorotation and the Flat Spin. N. A. C. A. Technical Report No. 273 (1927).

Reference 4.

Loeser, jr., Oscar E.: Pressure Distribution Tests on PW-9 Wing Models from −18° through 90° Angle of Attack. N. A. C. A. Technical Report No. 296 (1928).

Glauert, H.: The Rotation of an Aerofoil about a Fixed Axis. B. A. C. A. Reports and Memoranda No. 6 8 (1919).

Irving, H. B., and Batson, A. S.: The Effects of Stagger and Gap on the Aerodynamic Properties of Biplanes at Large Angles of Incidence. B. A. C. A. Reports and Memoranda No. 1064 (1927).

Gates, S. B., and Bryant, L. W.: The Spinning of Aeroplanes. B. A. C. A. Reports and Memoranda No. 1001 (1926).

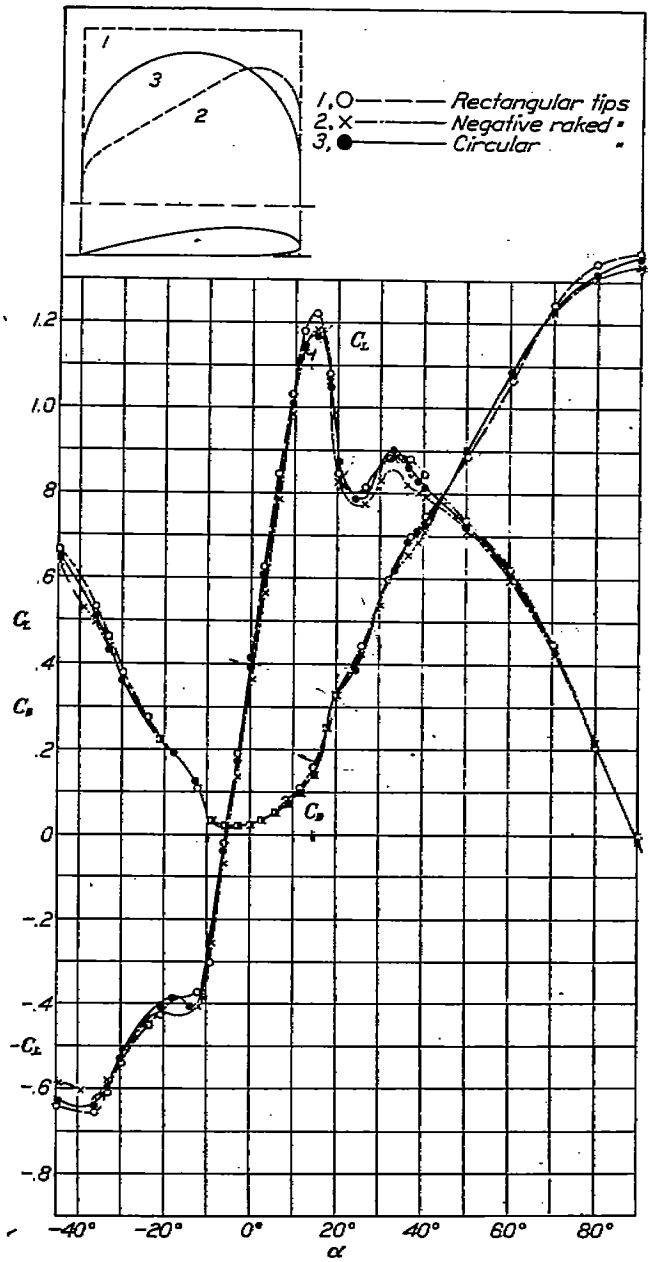

FIGURE 2.—Monoplane wing. Tip shape effect. Clark Y. 5-inch chord. A. R. 6

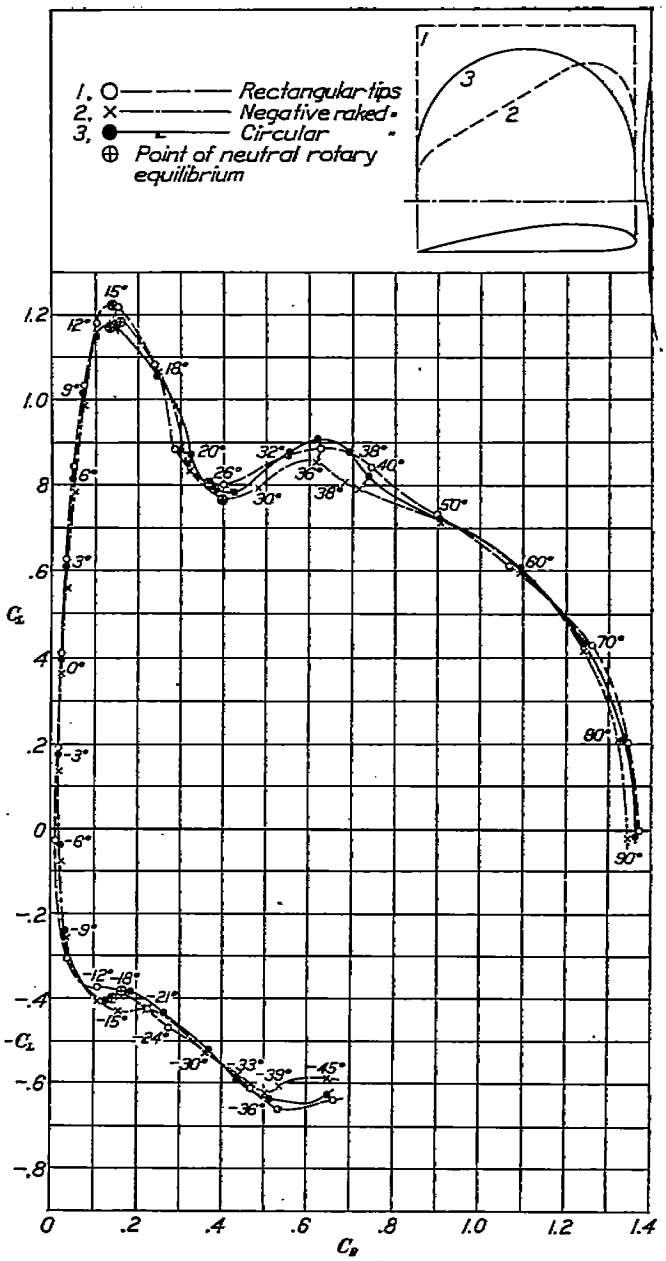

FIGURE 3.—Monoplane wings. Tip shape effect. Polars. Clark Y. 5-inch chord. A. R. 6

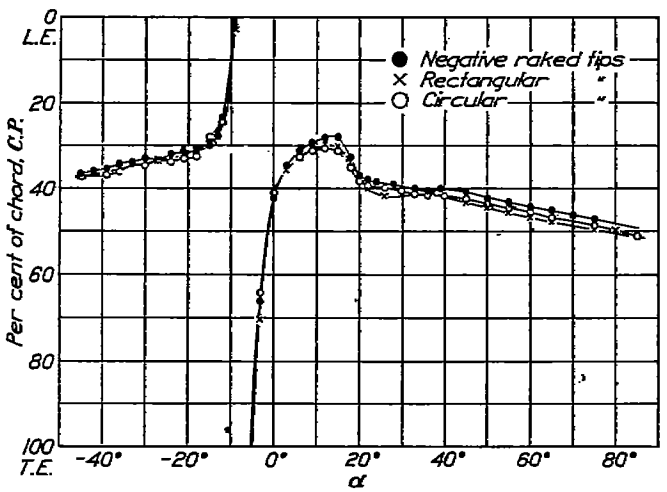

FIGURE 4.—Monoplane wings. Tip shape effect. Clark Y. 5-inch chord. A. R. 6

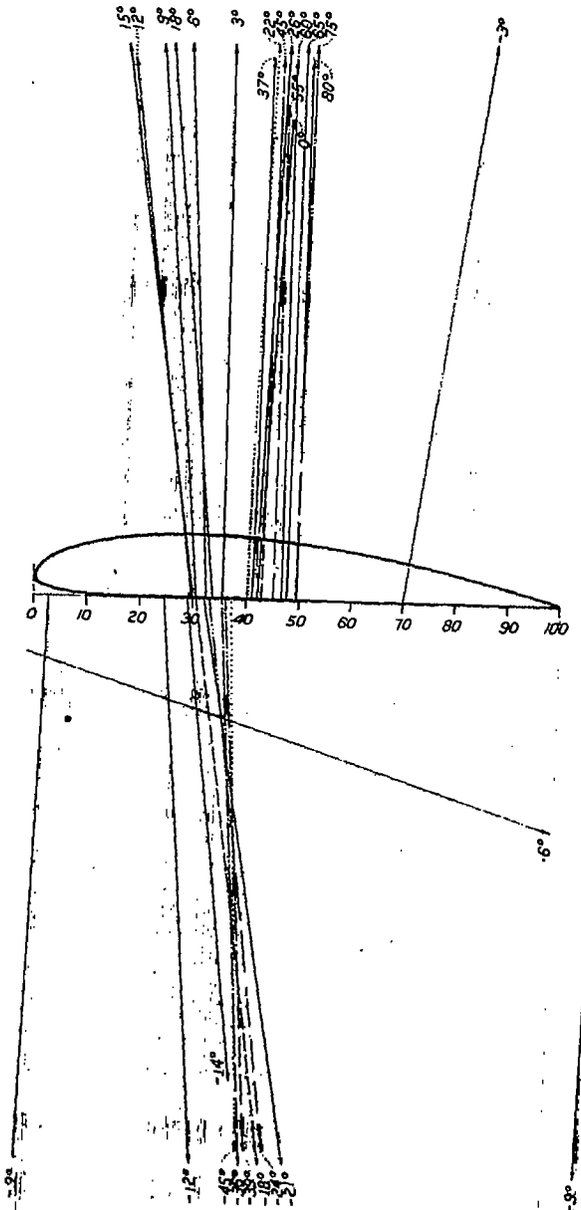

FIGURE 5.—Monoplane vector diagram. Clark Y. Rectangular tips. 5-inch chord. A. R. 6

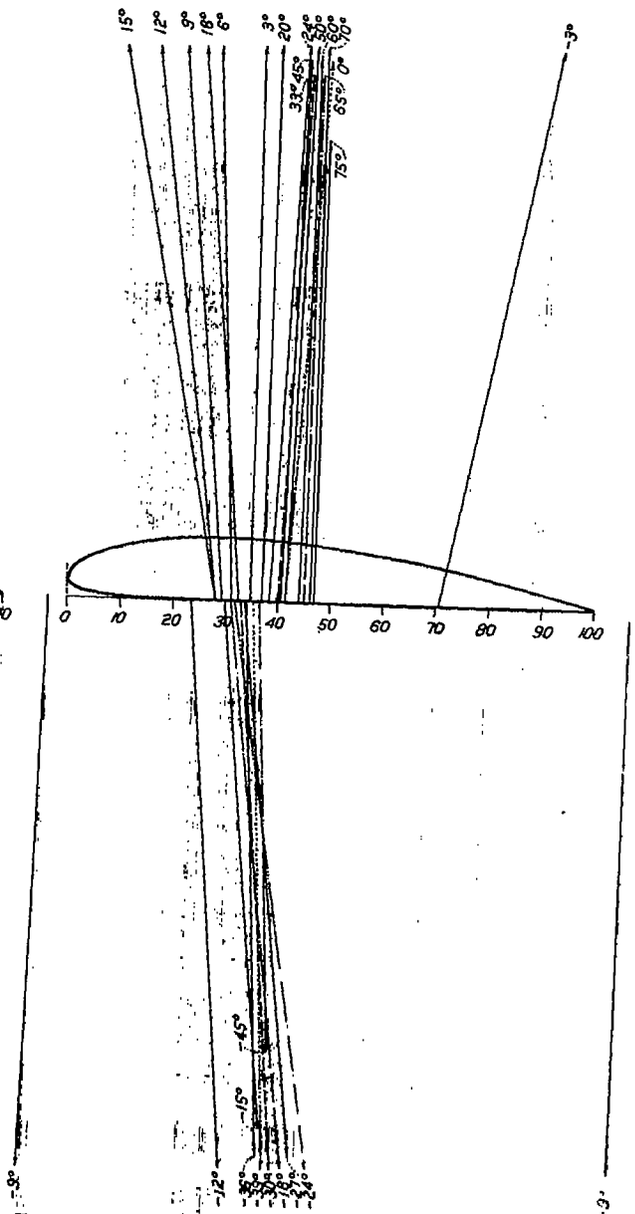

FIGURE 6.—Monoplane vector diagram. Clark Y. Negative raked tips. 5-inch chord. A. R. 6

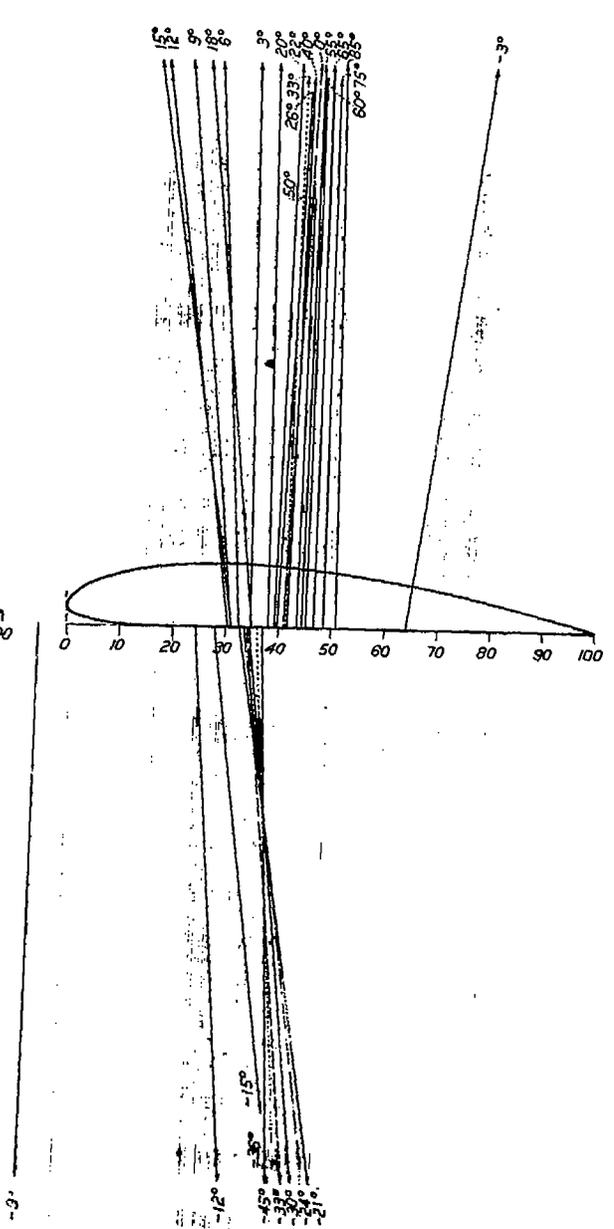

FIGURE 7.—Monoplane vector diagram. Clark Y. Circular tips. 5-inch chord. A. R. 6

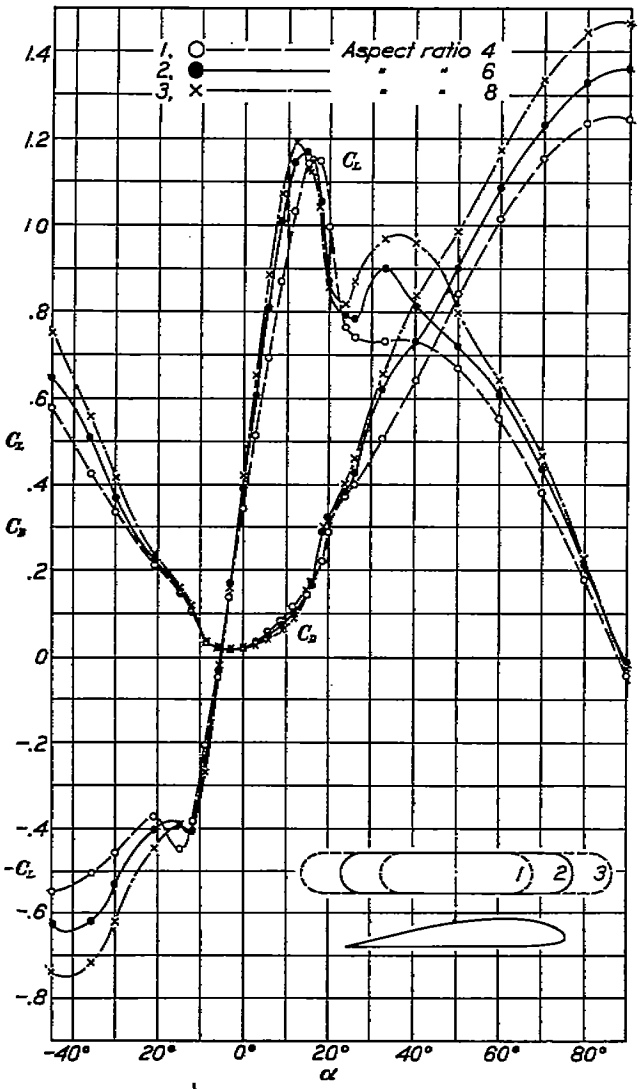

FIGURE 8.—Monoplane wings. Aspect ratio effect. Clark Y. Circular tips. 5-inch chord

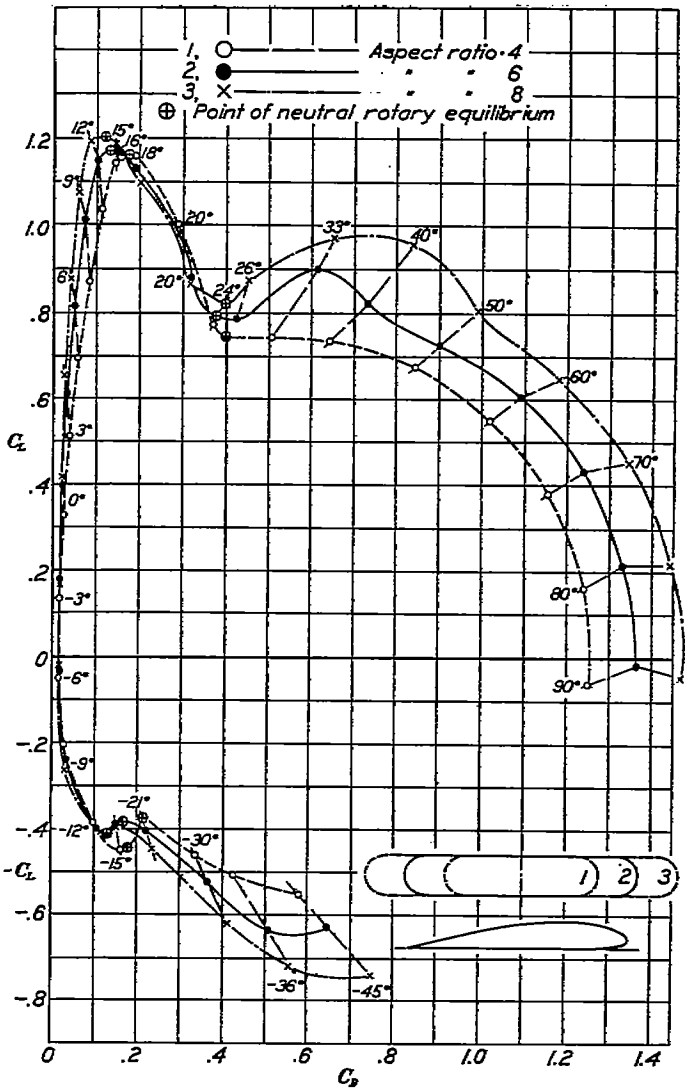

FIGURE 9.—Monoplane wings. Aspect ratio effect. Polars. Clark Y. Circular tips. 5-inch chord

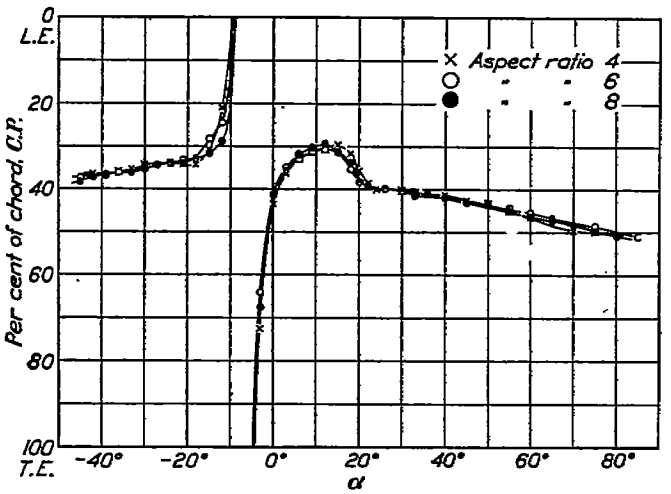

FIGURE 10.—Monoplane wings. Aspect ratio effect. Clark Y. Circular tips. 5-inch chord

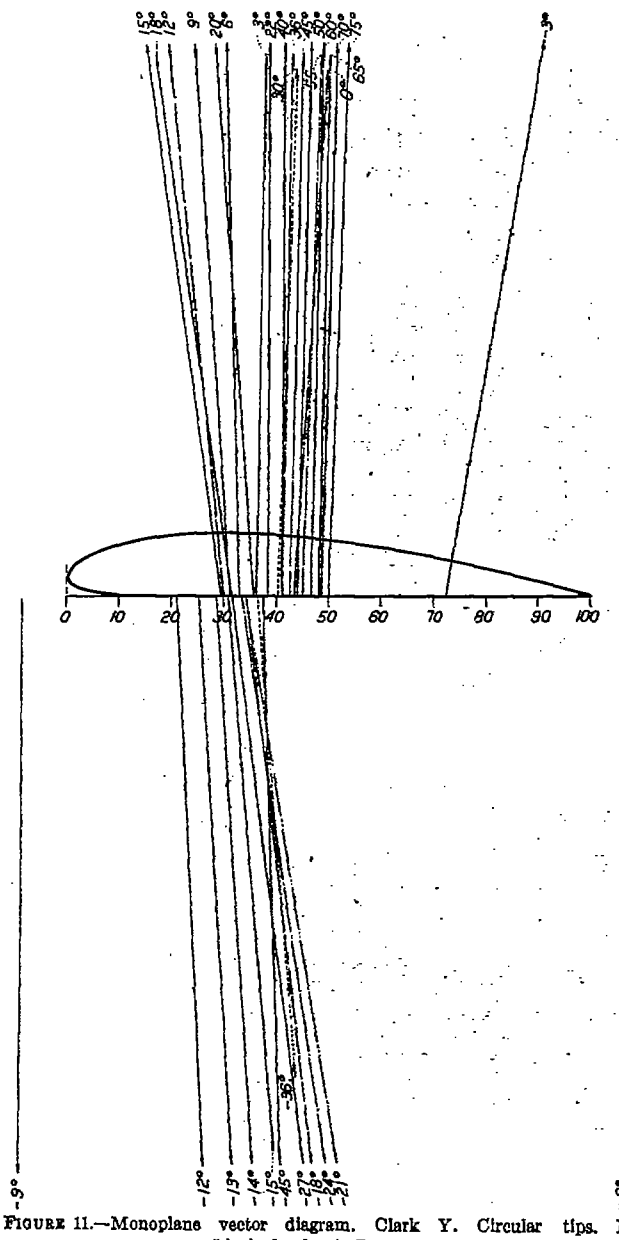

FIGURE 11.—Monoplane vector diagram. Clark Y. Circular tips. 5-inch chord. A. R. 4

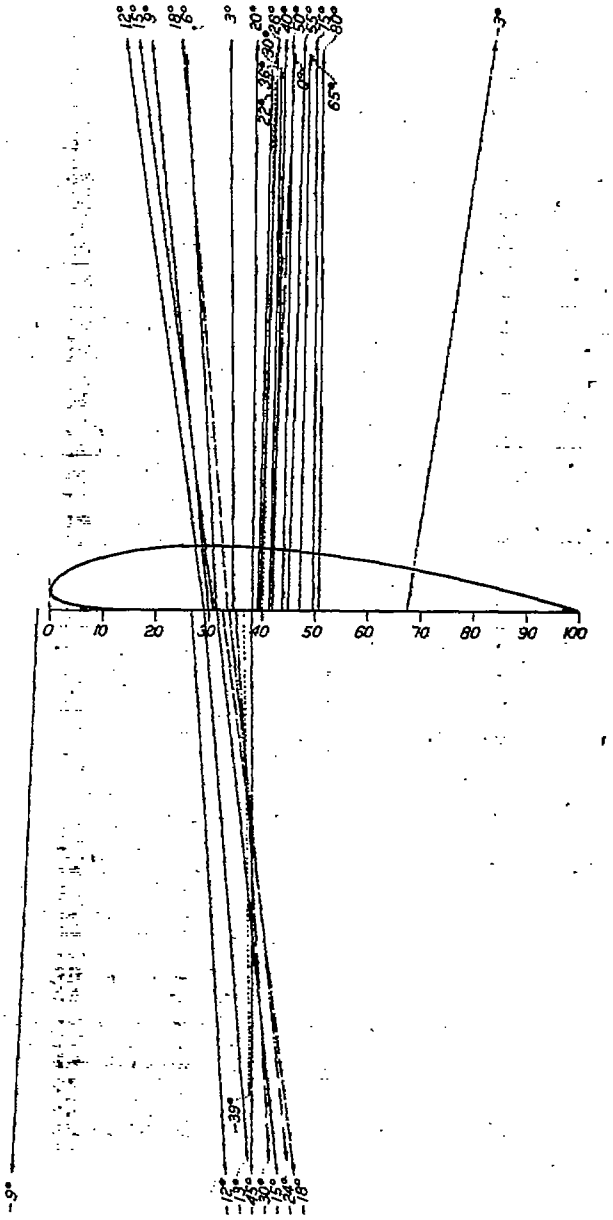

FIGURE 12.—Monoplane vector diagram. Clark Y. Circular tips 5-inch chord. A. R. 8

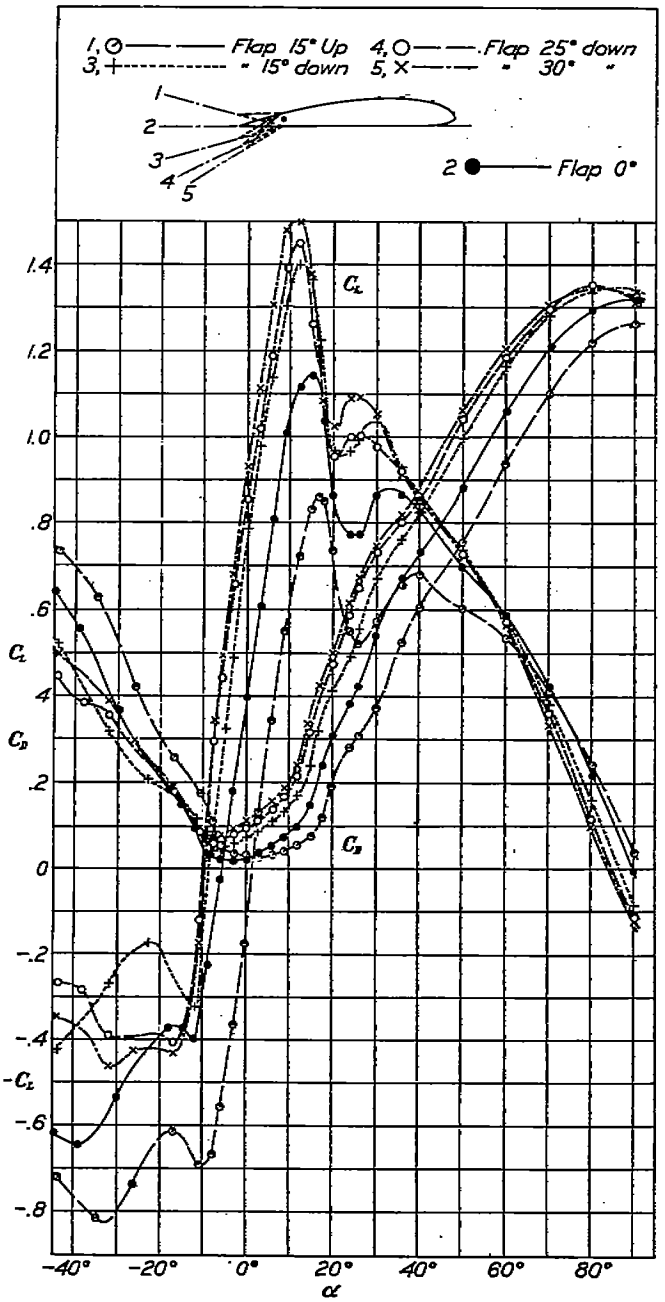

FIGURE 13.—Monoplane wings. Flap-setting effect. Clark Y. Flaps 20 per cent chord. Circular tips. 5-inch chord. A. R. 6

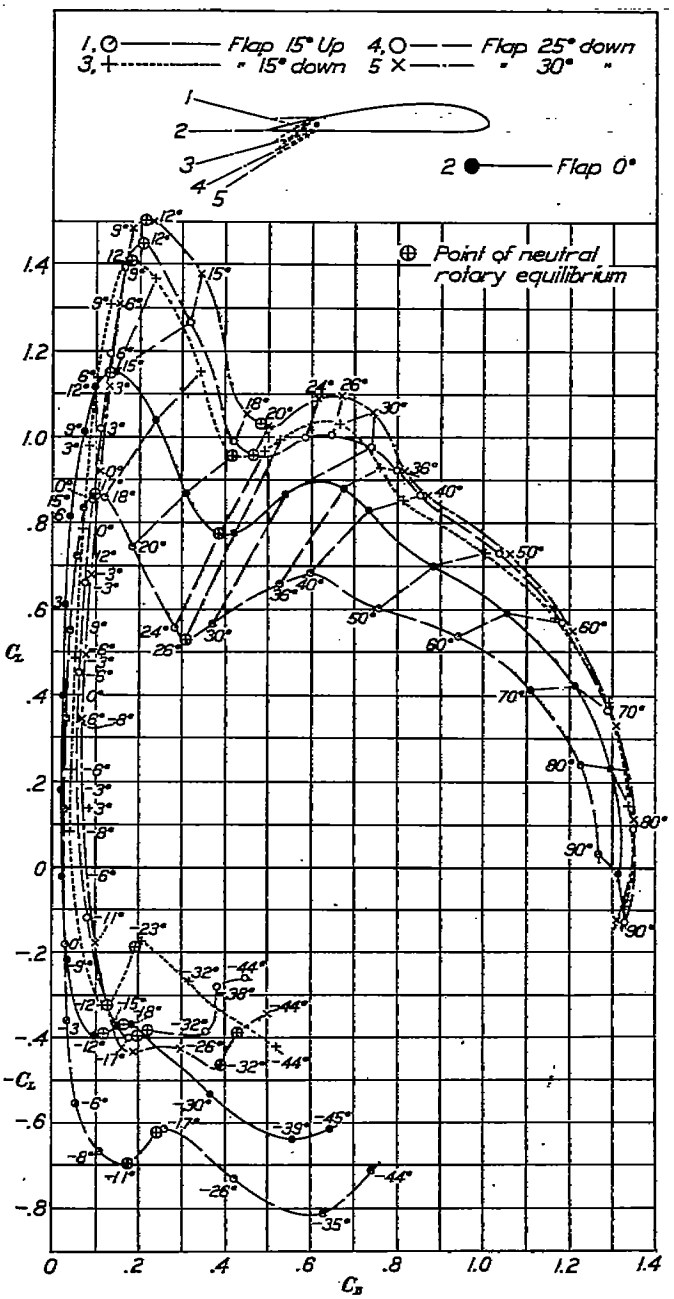

FIGURE 14.—Monoplane wings. Flap-setting effect. Polars. Clark Y. Flaps 20 per cent chord. Circular tips. 5-inch chord. A. R. 6

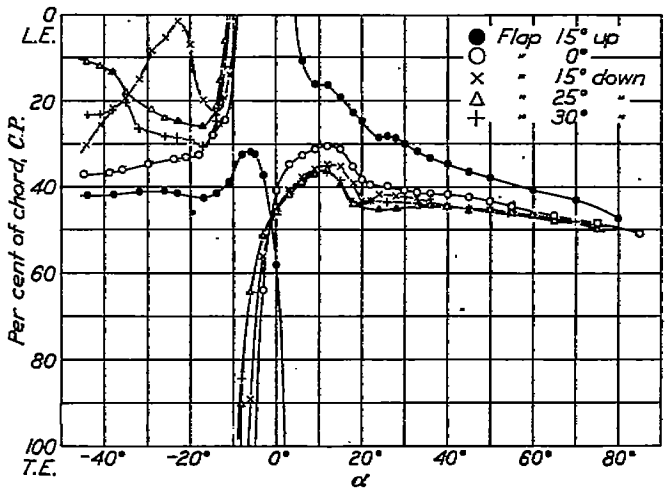

FIGURE 15.—Monoplane wings. Flap-setting effect. Clark Y. Flaps 20 per cent chord. Circular tips 5-inch chord. A. R. 6

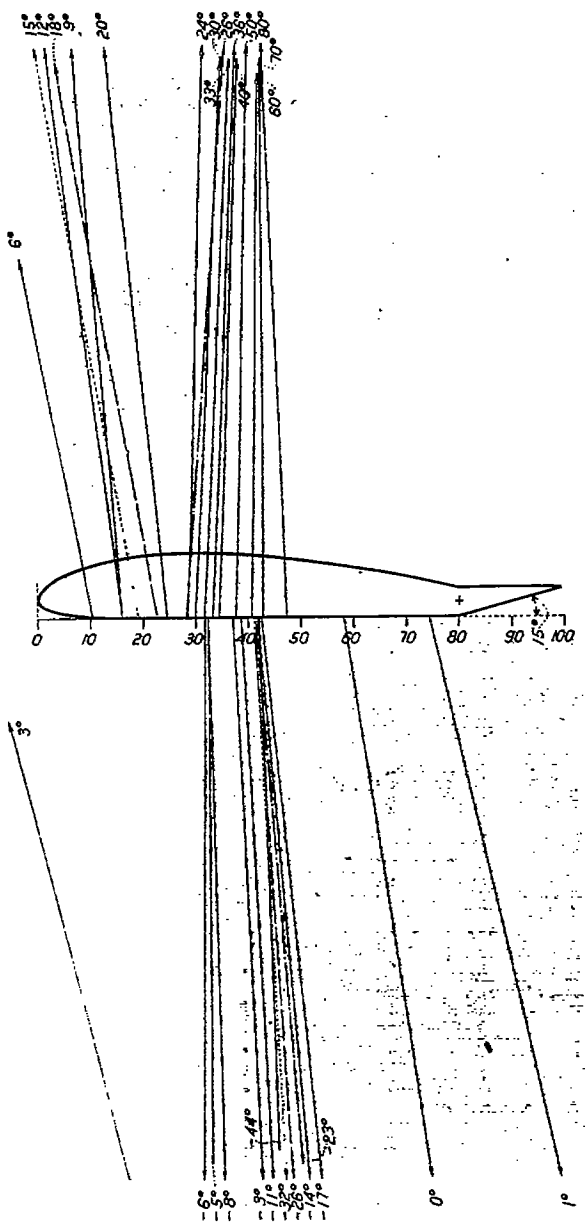

FIGURE 16.—Monoplane vector diagram. Clark Y. Circular tips. 5-inch chord. A. R. 6. Flap up 15°

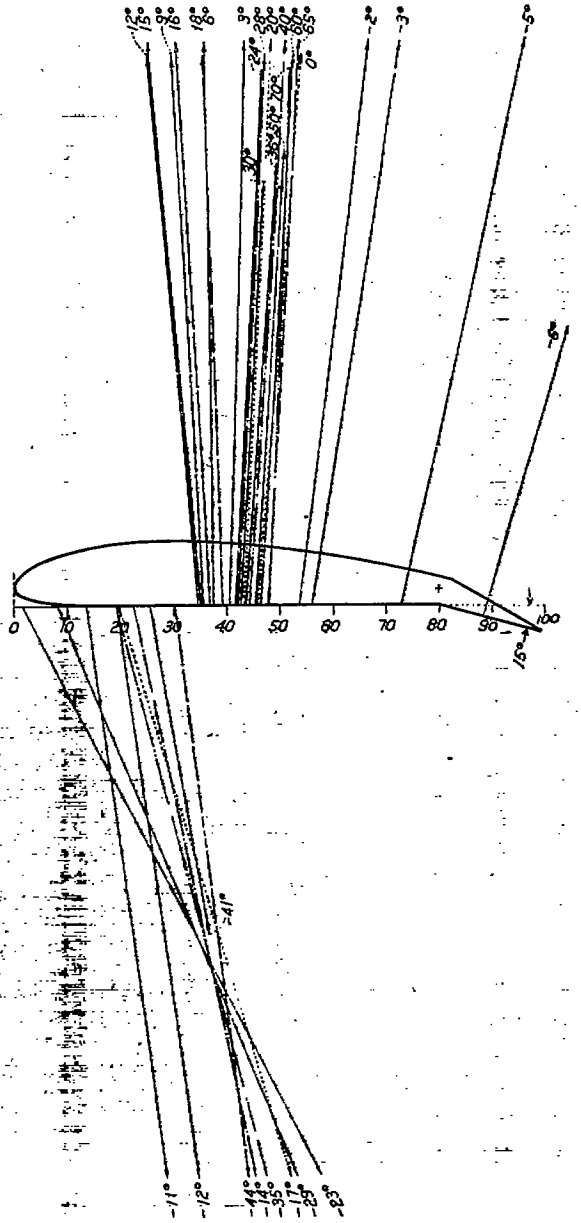

FIGURE 17.—Monoplane vector diagram. Clark Y. Circular tips. 5-inch chord. A. R. 6. Flap down 15°

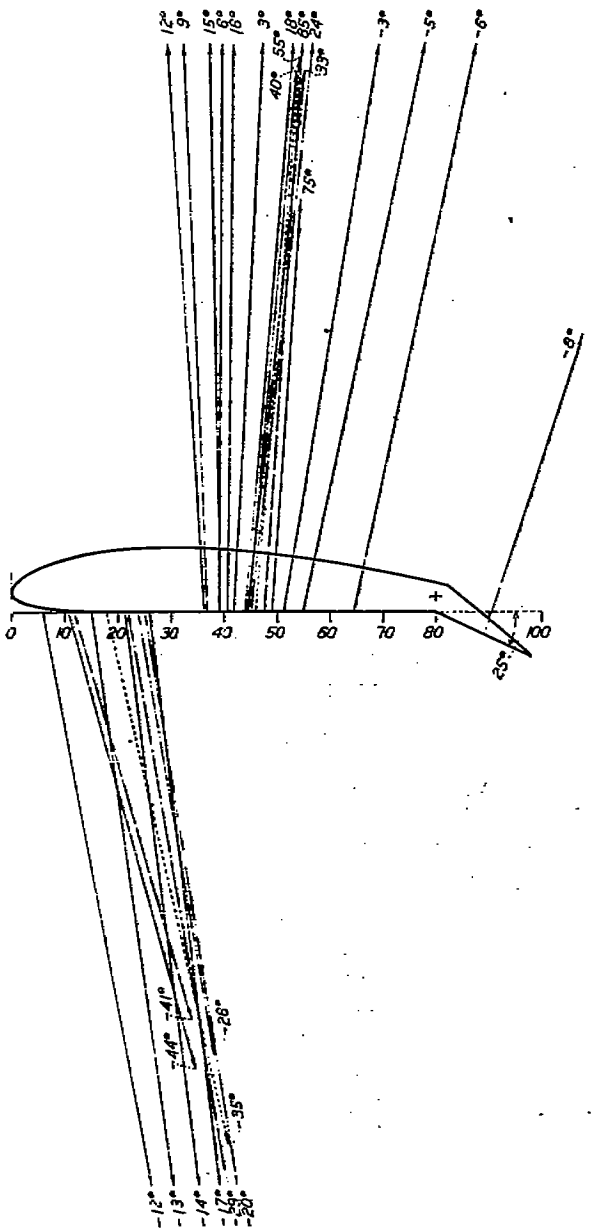

FIGURE 18.—Monoplane vector diagram. Clark Y. Circular tips. 5-inch chord. A. R. 6. Flap down 25°

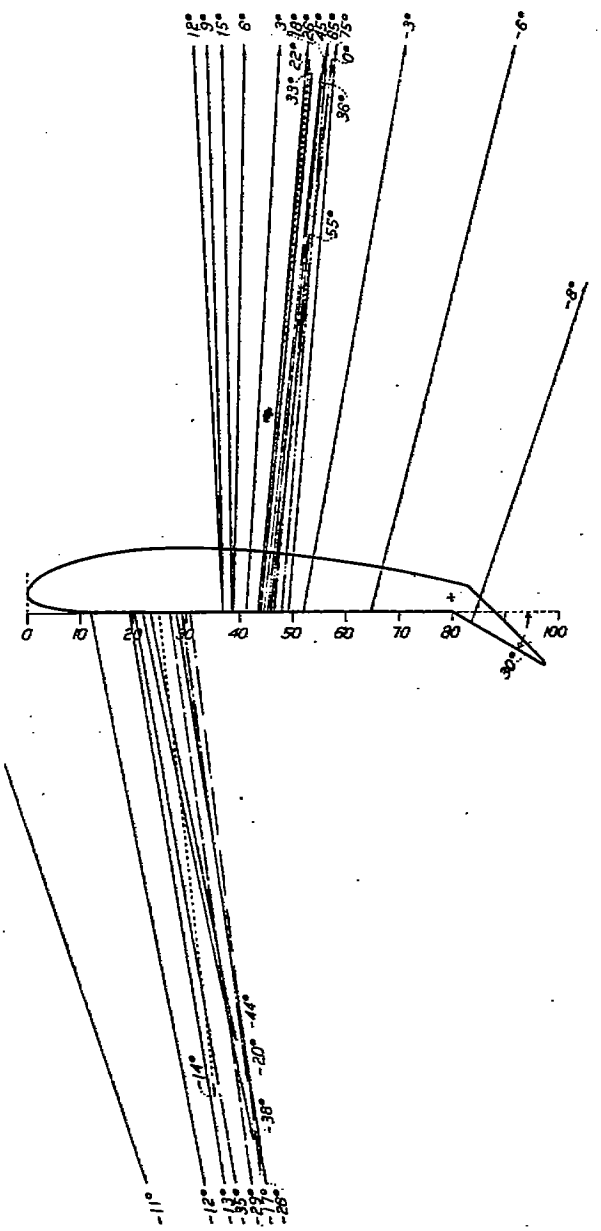

FIGURE 19.—Monoplane vector diagram. Clark Y. Circular tips. 5-inch chord. A. R. 6. Flap down 30°

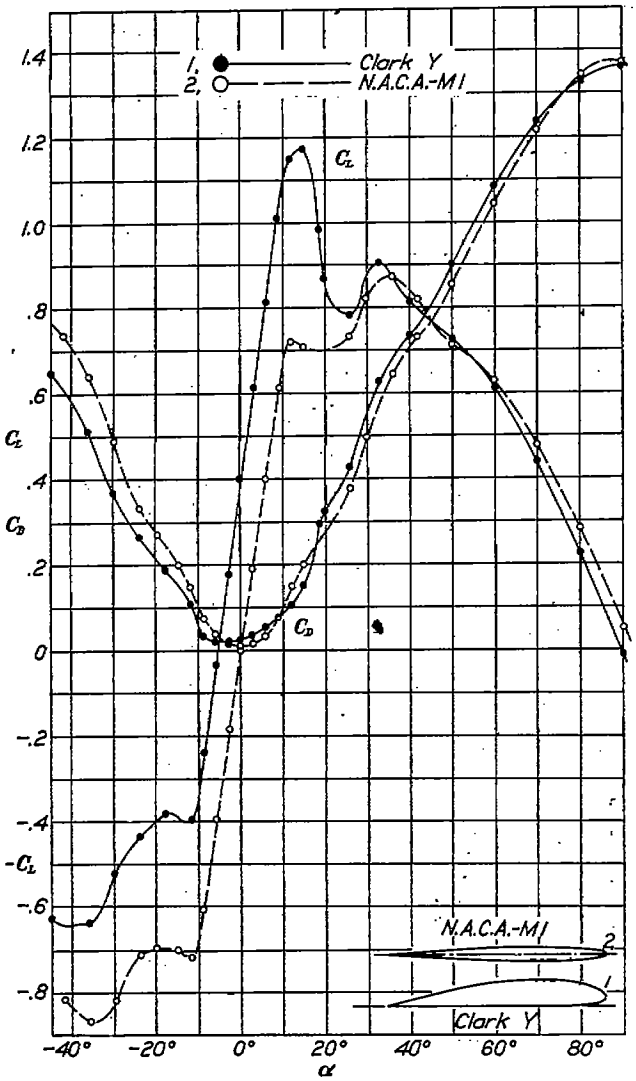

FIGURE 20.—Monoplane wings. Profile effect. Clark Y. and N. A. C. A.-M1. Circular tips. 5-inch chord. A. R. 6

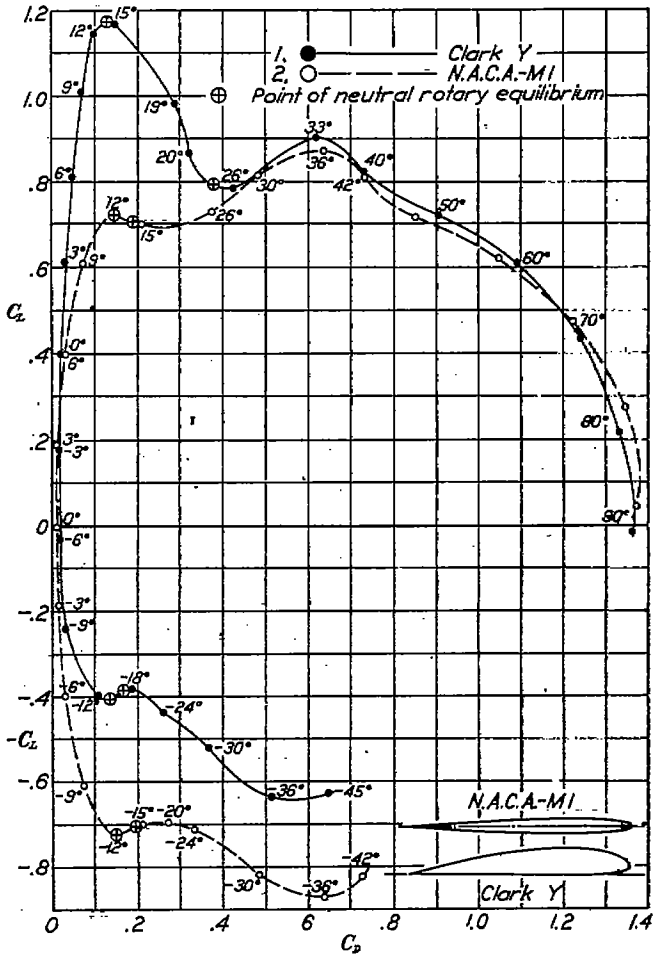

FIGURE 21.—Monoplane wings. Profile effect. Polars. Clark Y. and N. A. C. A.-M1. Circular tips. 5-inch chord. A. R. 6

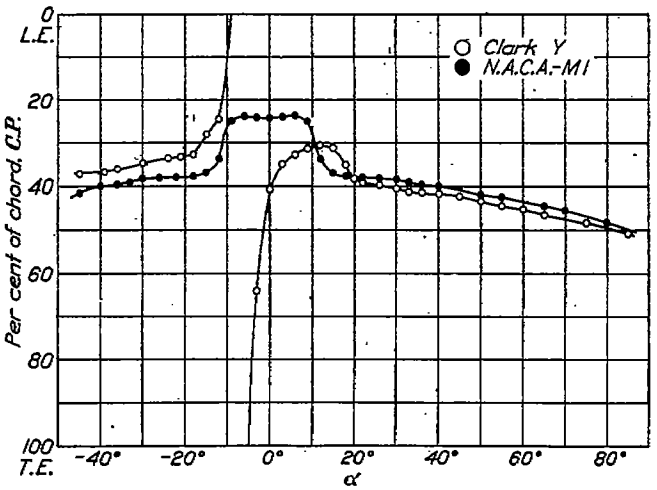

FIGURE 22.—Monoplane wings. Profile effect. Clark Y. and N. A. C. A.-M1. Circular tips. 5-inch chord. A. R. 6

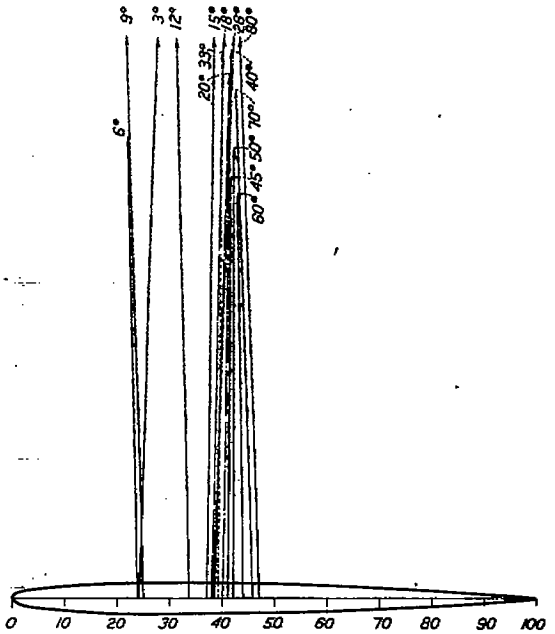

FIGURE 23.—Monoplane vector diagram. N. A. C. A.-M1. Circular tips. 5-inch chord. A. R. 6

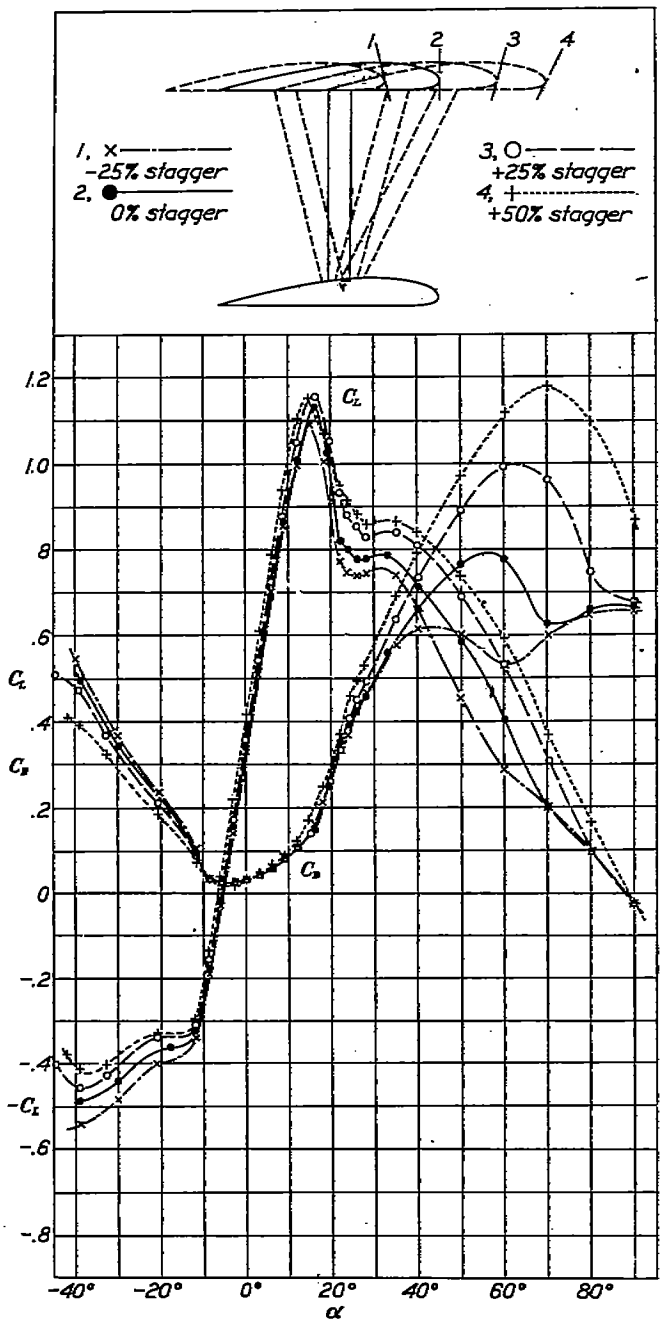

[FIGURE 24.—Biplane wings. Stagger effect. Clark Y. Circular tips. 5-inch chord. A. R. 6. Gap/chord=1. Decalage, 0°

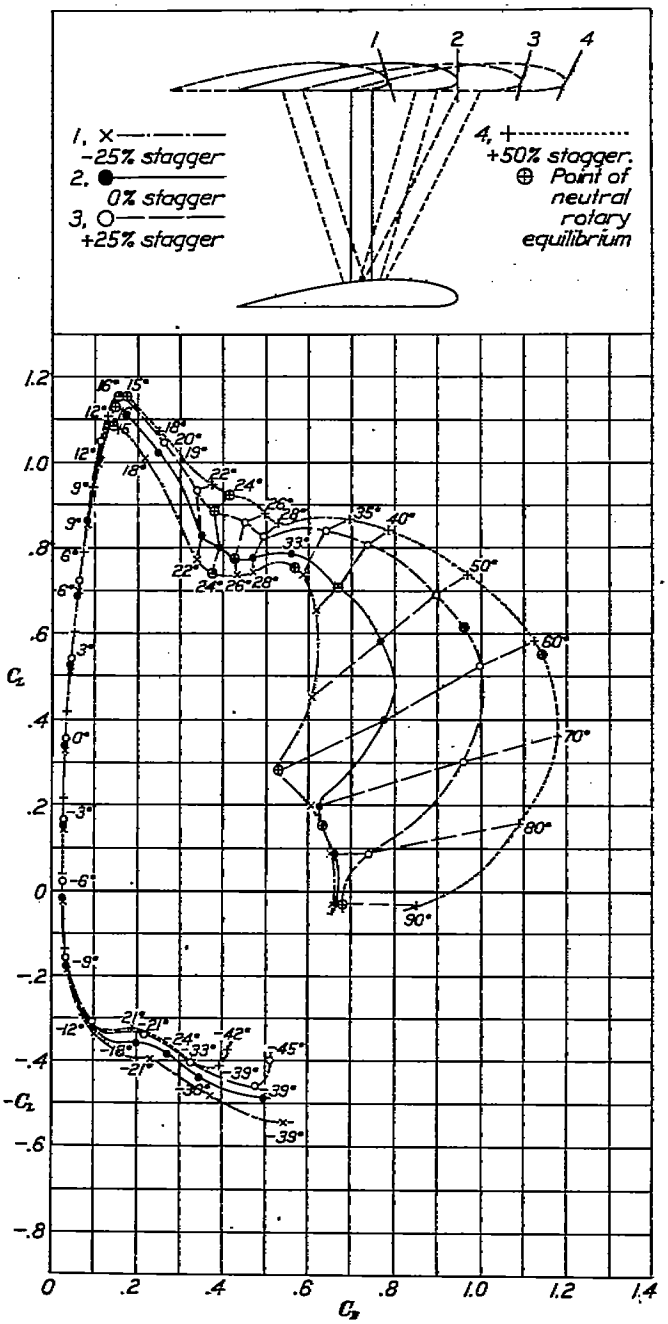

FIGURE 25.—Biplane wings. Stagger effect. Polars. Clark Y. Circular tips. 5-inch chord. A. R. 6. Gap/chord=1. Decalage, 0°

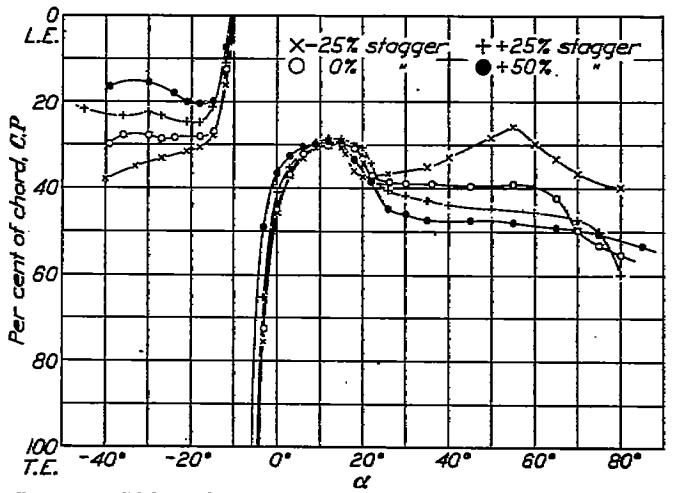

FIGURE 26.—Biplane wings. Stagger effect. Clark Y. Circular tips. 5-inch chord. A. R. 6. Gap/chord=1. Decalage, 0°

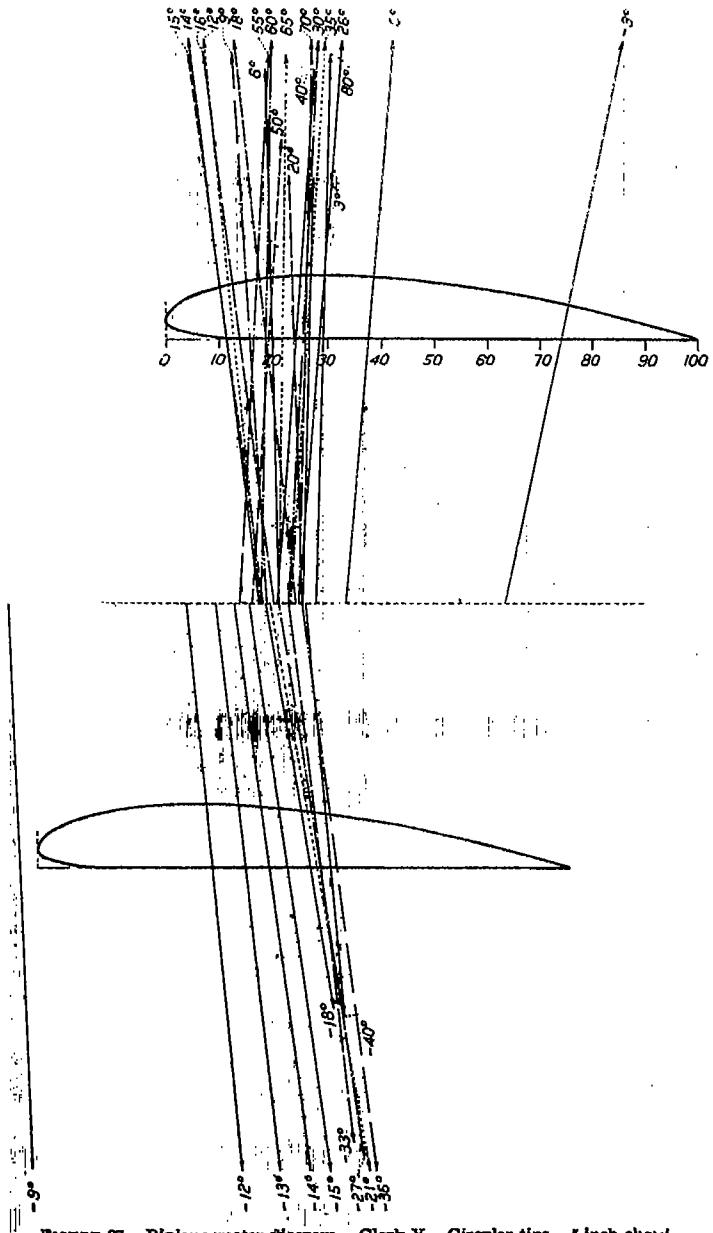

FIGURE 27.—Biplane vector diagram. Clark Y. Circular tips. 5-inch chord. A. R. 6. Gap/chord=1. Decalage, 0°. Stagger, −25 per cent chord

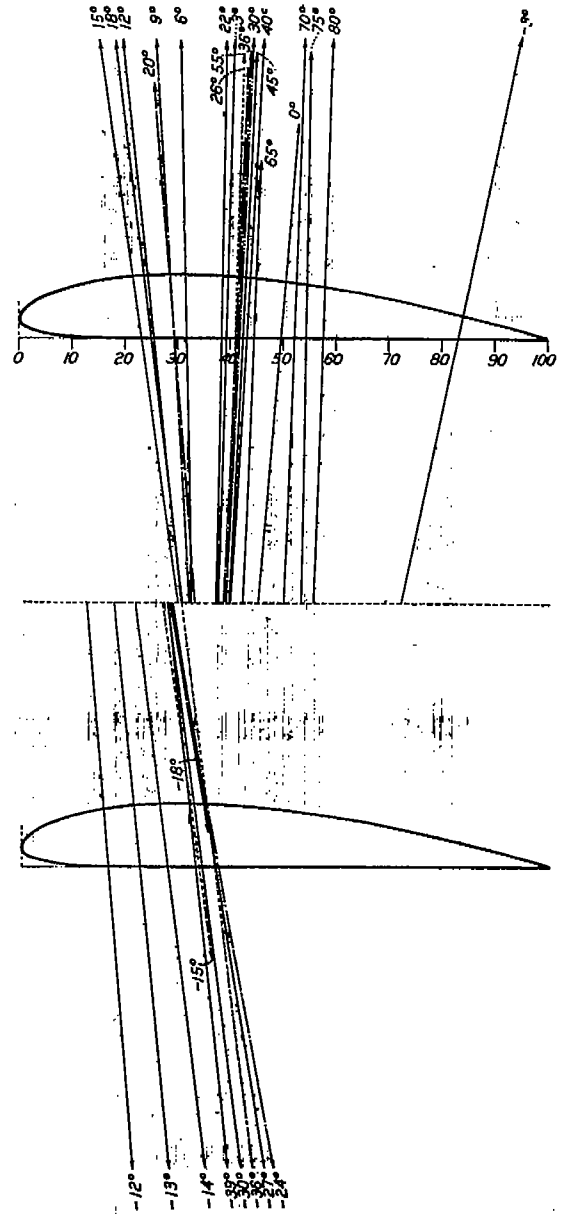

FIGURE 28.—Biplane vector diagram. Clark Y. Circular tips. 5-inch chord. A. R. 6. Gap/chord=1. Decalage, 0°. Stagger, 0.

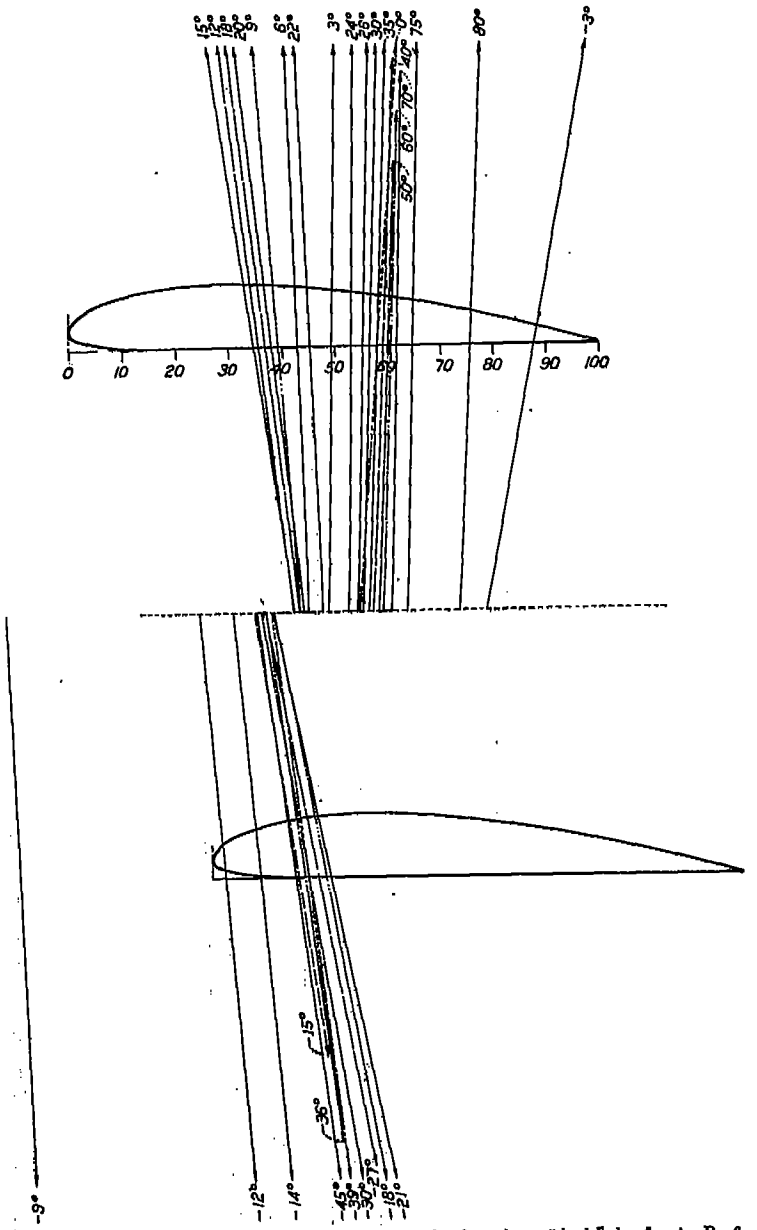

FIGURE 29.—Biplane vector diagram. Clark Y. Circular tips. 5-inch chord. A. R. 6. Gap/chord=1. Decalage, 0°. Stagger, +25 per cent chord

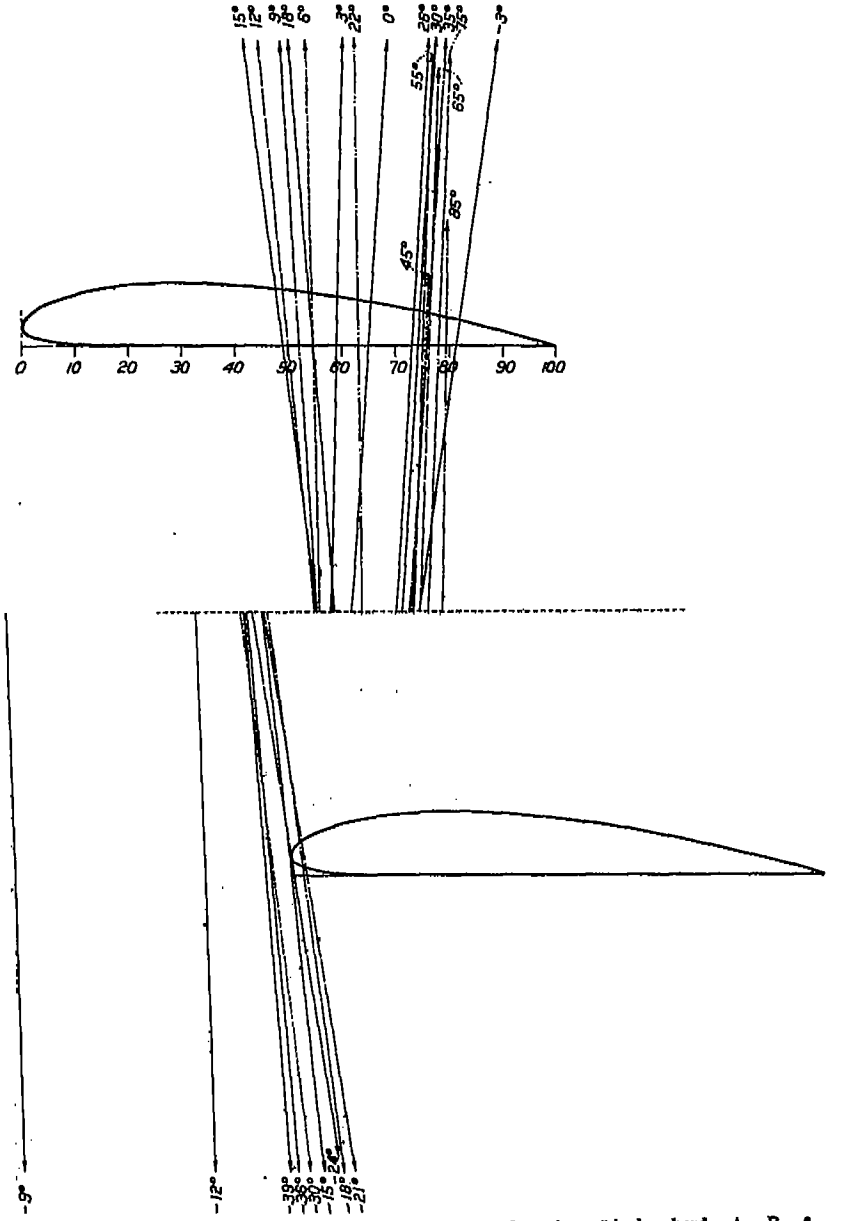

FIGURE 30.—Biplane vector diagram. Clark Y. Circular tips. 5-inch chord. A. R. 6. Gap/chord=1. Decalage, 0°. Stagger, +50 per cent chord

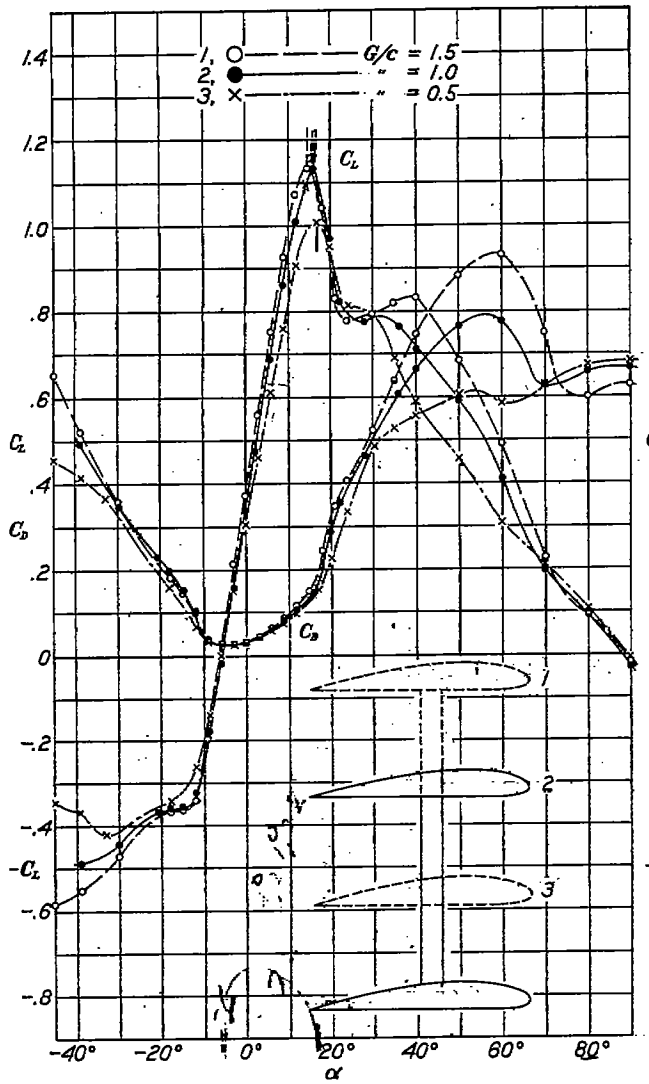

FIGURE 31.—Biplane wings. Gap effect. Clark Y. Circular tips. 5-inch chord. A. R. 6. Decalage, 0°. Stagger, 0

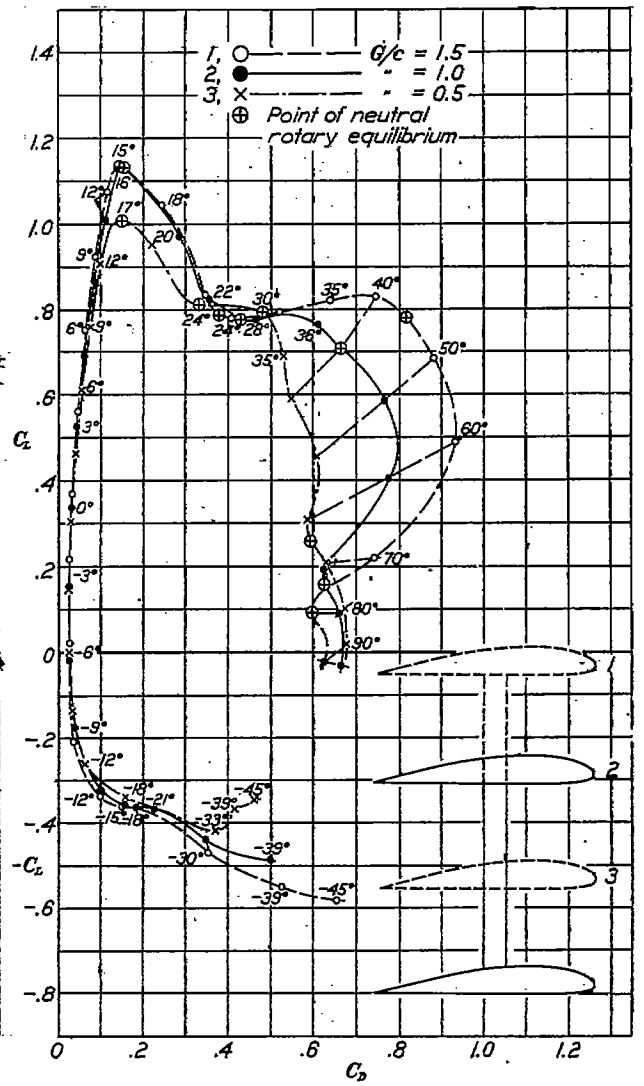

FIGURE 32.—Biplane wings. Gap effect. Polars. Clark Y. Circular tips. 5-inch chord. A. R. 6. Decalage, 0°. Stagger, 0

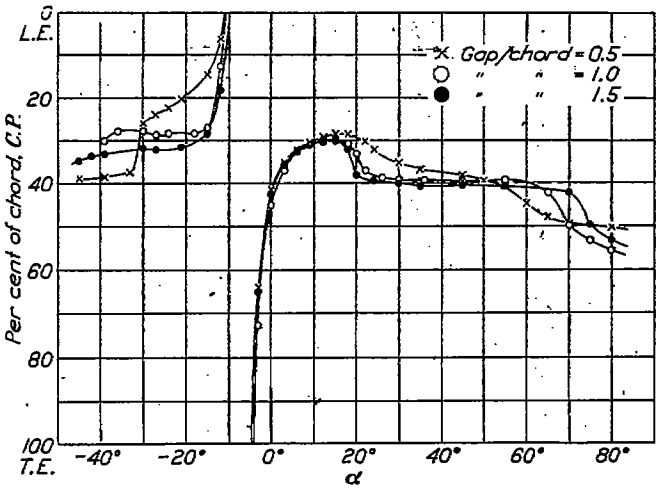

FIGURE 33.—Biplane wings. Gap effect. Clark Y. Circular tips. 5-inch chord. A. R. 6. Decalage, 0°. Stagger, 0

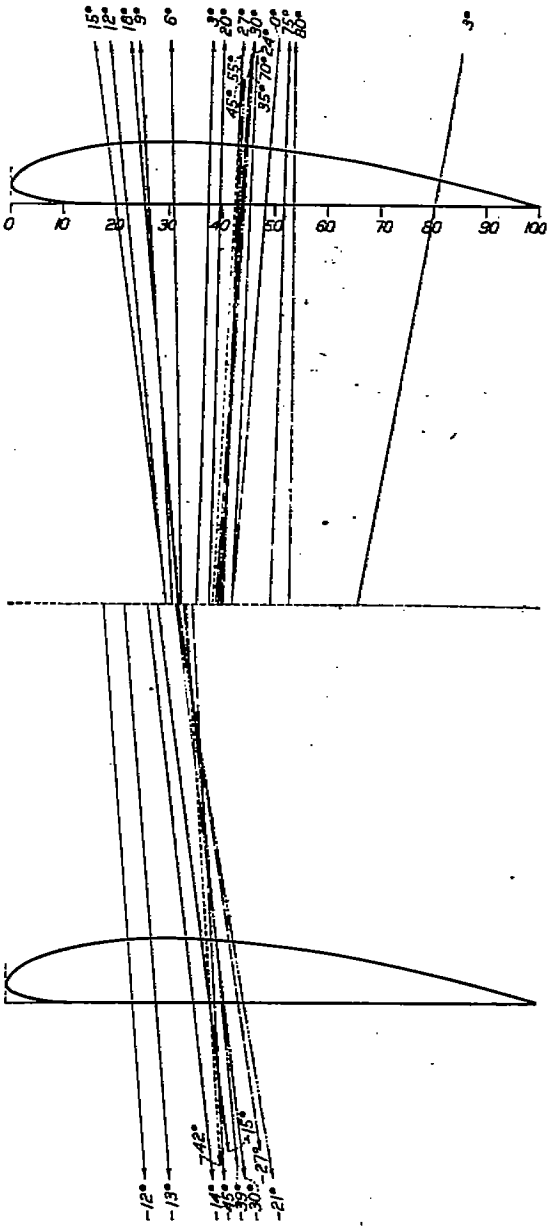

FIGURE 34.—Biplane vector diagram. Clark Y. Circular tips. 5-inch chord. A. R. 6. Gap/chord=1.5. Decalage, 0°. Stagger, 0

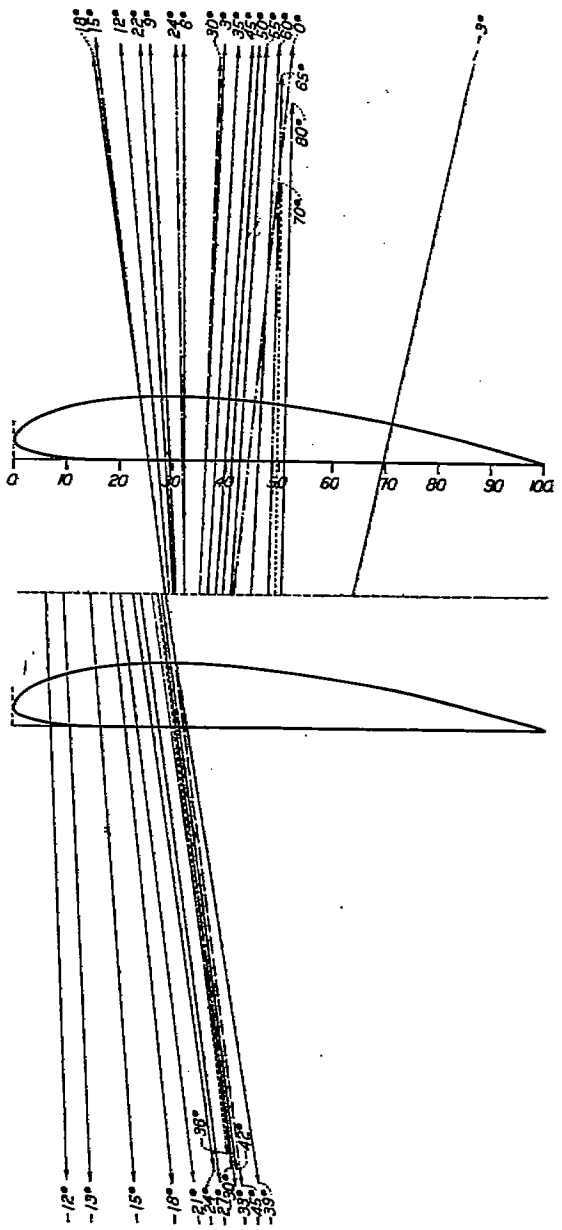

FIGURE 35.—Biplane vector diagram. Clark Y. Circular tips. 5-inch chord. A. R. 6. Gap/chord=0.5. Decalage, 0°. Stagger, 0

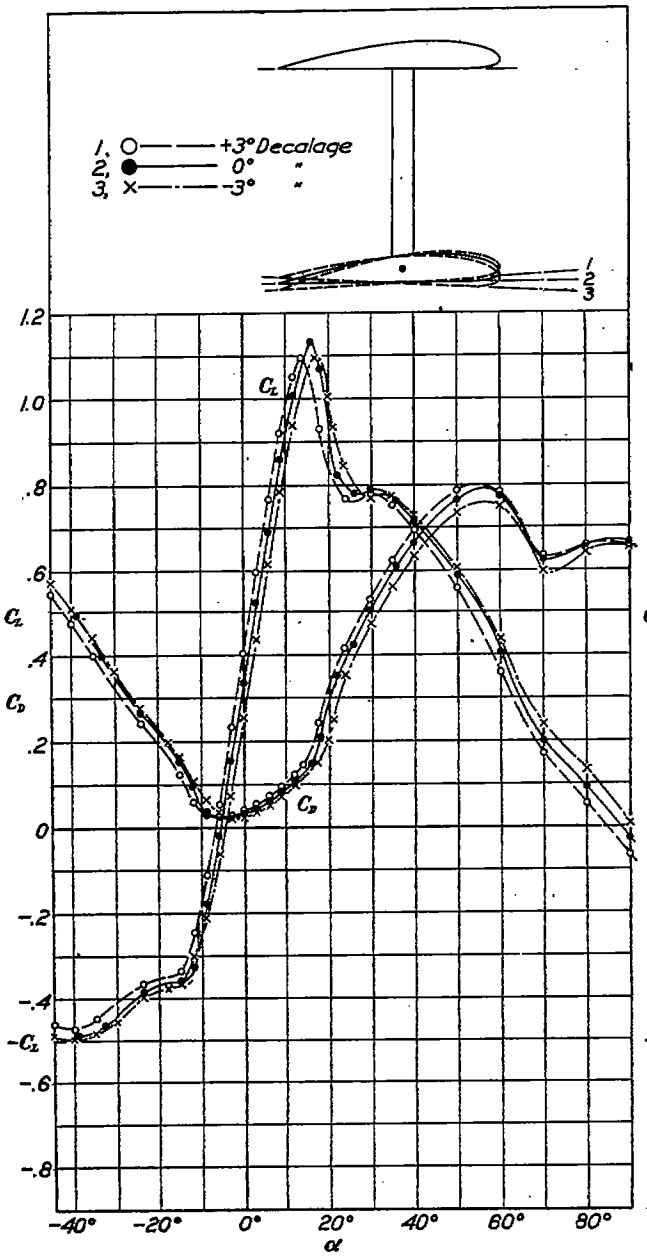

FIGURE 36.—Biplane wings. Decalage effect. Clark Y. Circular tips. 5-inch chord. A. R. 6. Gap/chord=1. Stagger, 0

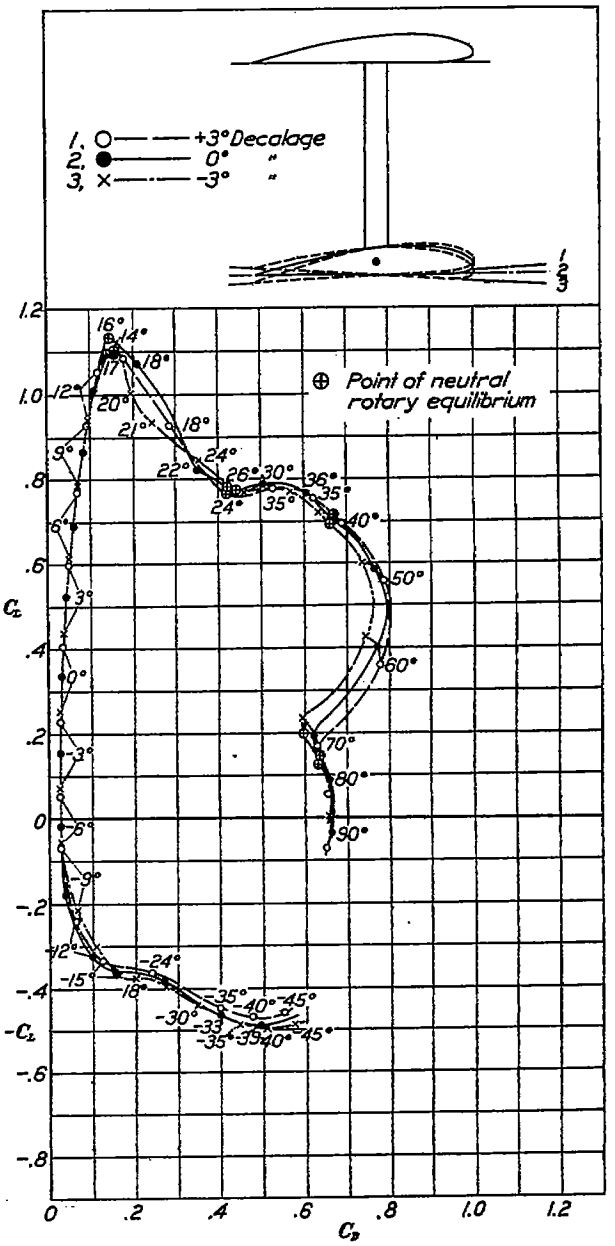

FIGURE 37.—Biplane wings. Decalage effect. Polars. Clark Y. Circular tips. 5-inch chord. A. R. 6. Gap/chord=1. Stagger, 0

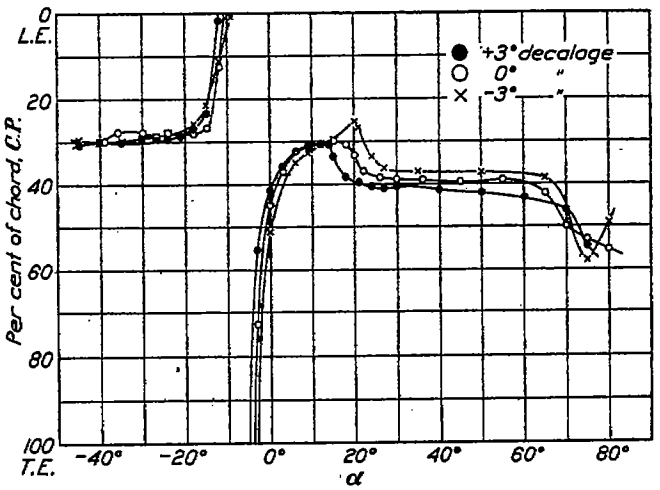

FIGURE 38.—Biplane wings. Decalage effect. Clark Y. Circular tips. 5-inch cord. A. R. 6. Gap/chord=1. Stagger, 0

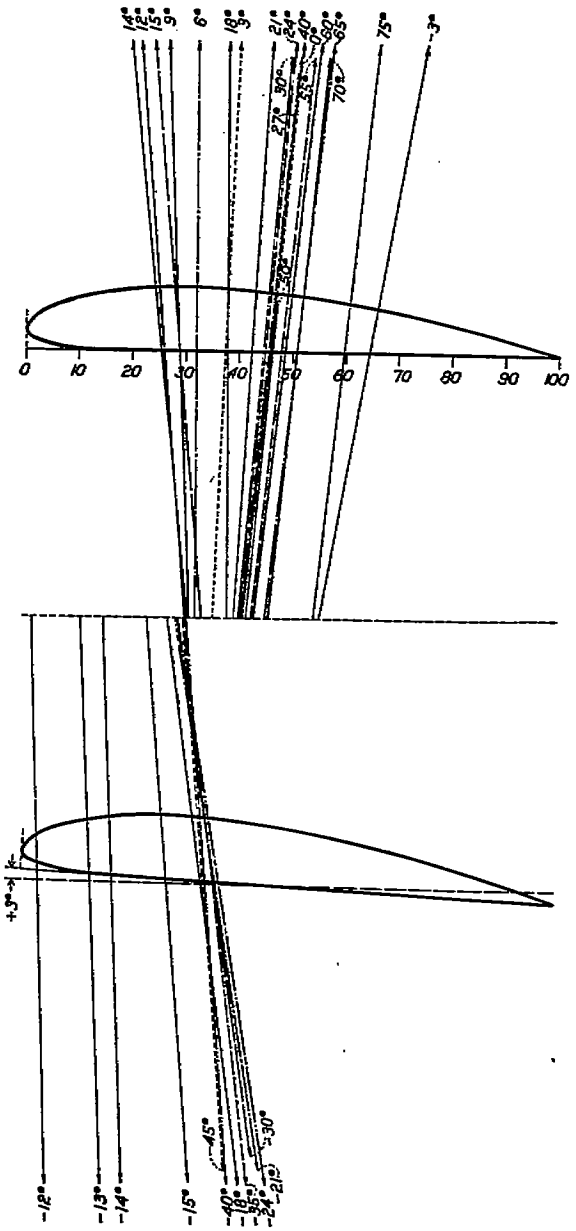

FIGURE 39.—Biplane vector diagram. Clark Y. Circular tips. 5-inch chord. A. R. 6. Gap/chord=1. Decalage, +3°. Stagger, 0

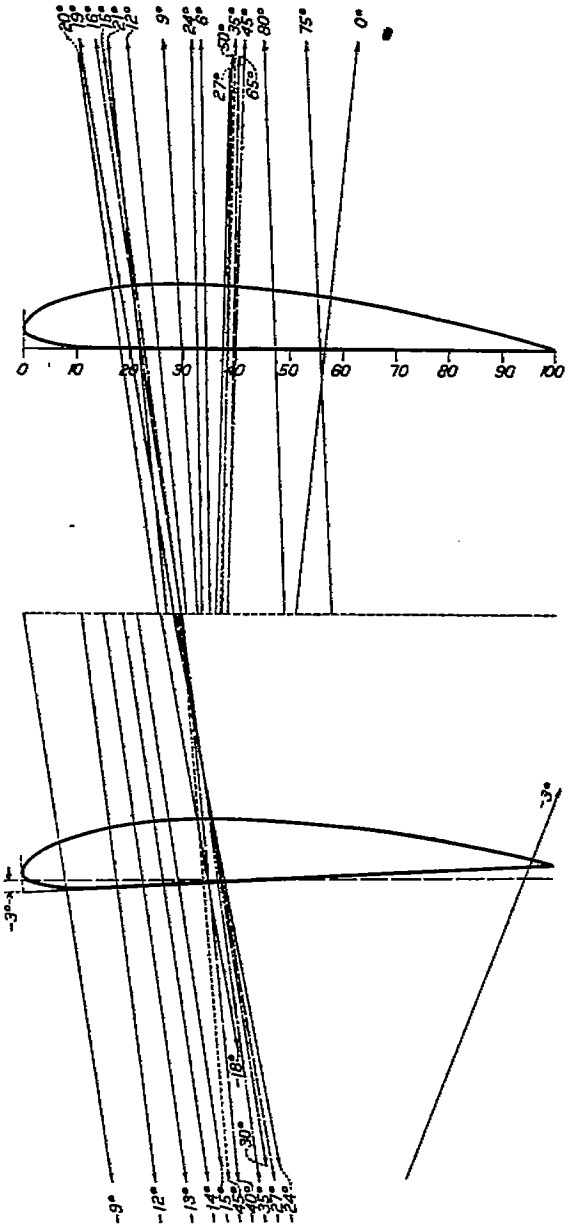

FIGURE 40.—Biplane vector diagram. Clark Y. Circular tips 5-inch chord. A. R. 6. Gap/chord=1. Decalage, −3°. Stagger, 0

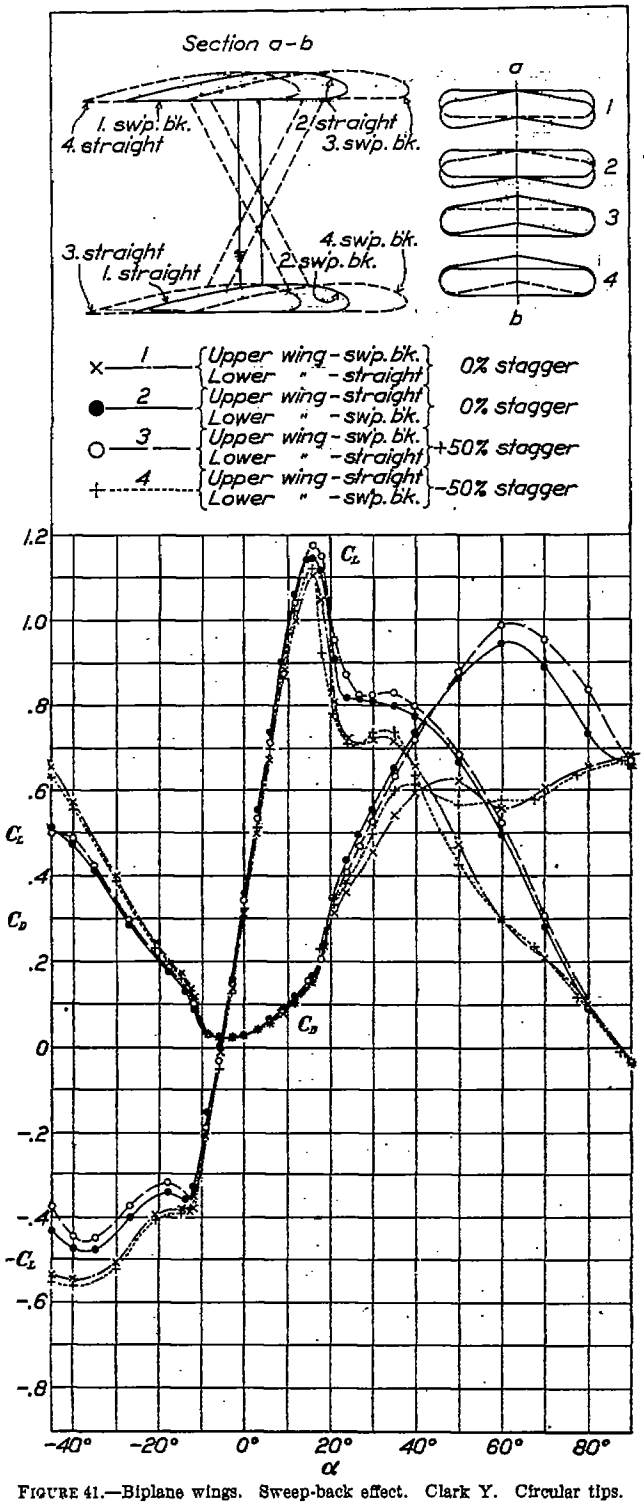

FIGURE 41.—Biplane wings. Sweep-back effect. Clark Y. Circular tips. 5-inch chord. A. R. 6. Gap/chord=1. Decalage, 0°

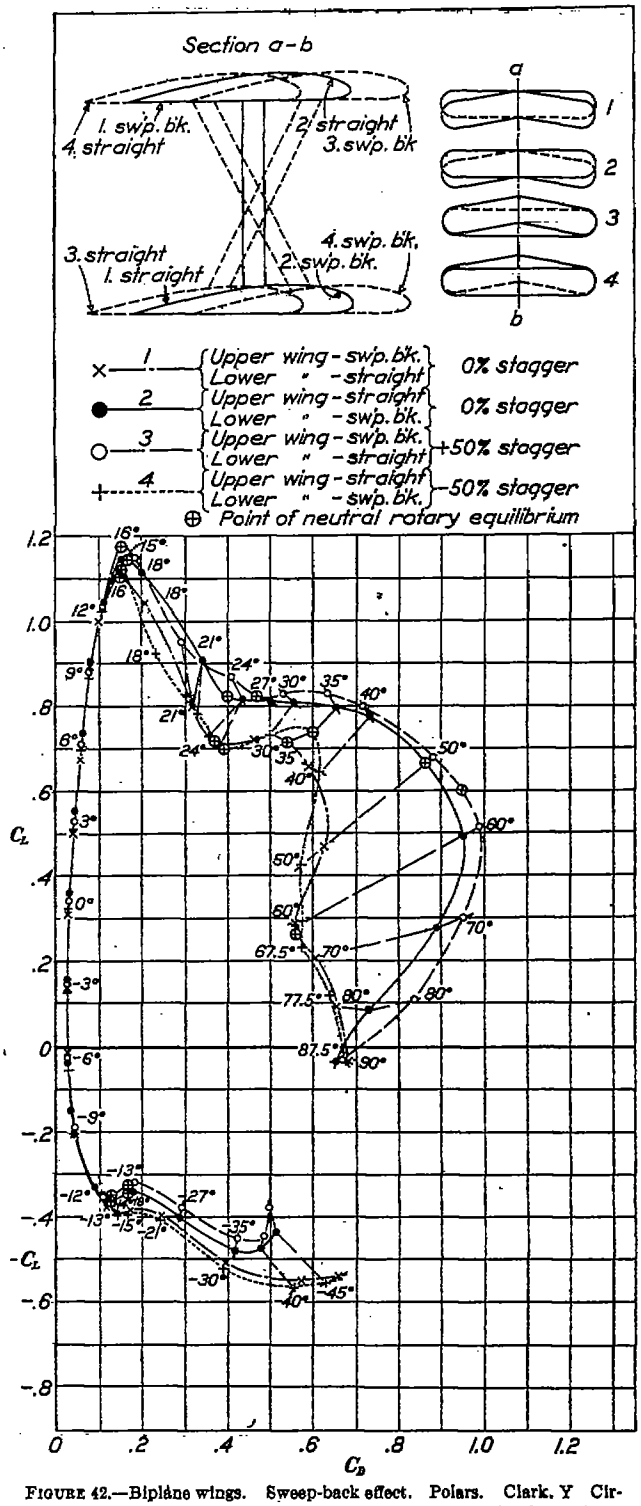

FIGURE 42.—Biplane wings. Sweep-back effect. Polars. Clark. Y Circular tips. 5-inch chord. A. R. 6. Gap/chord=1. Decalage 0°

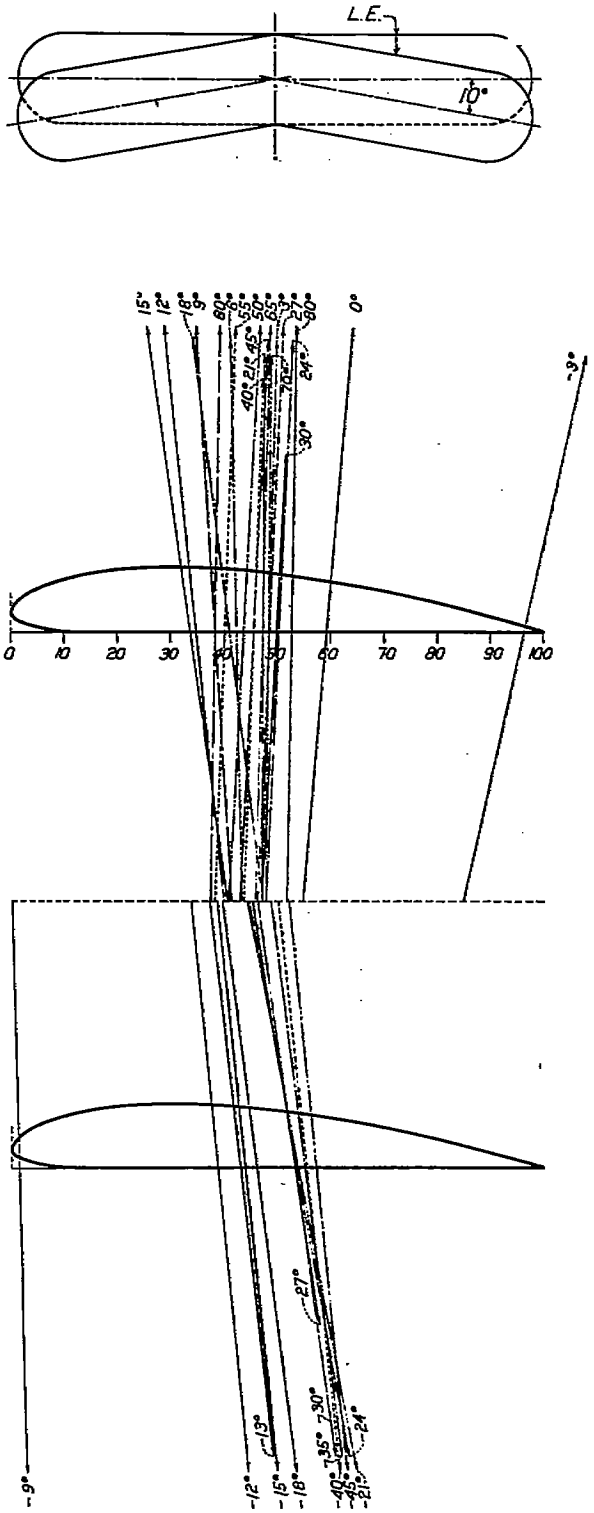

FIGURE 43.—Biplane vector diagram. Clark Y. Upper wing, swept back. Lower wing, straight. Circular tips. 5-inch chord. A. R. 6. Gap/chord=1. Decalage, 0°. Stagger, 0

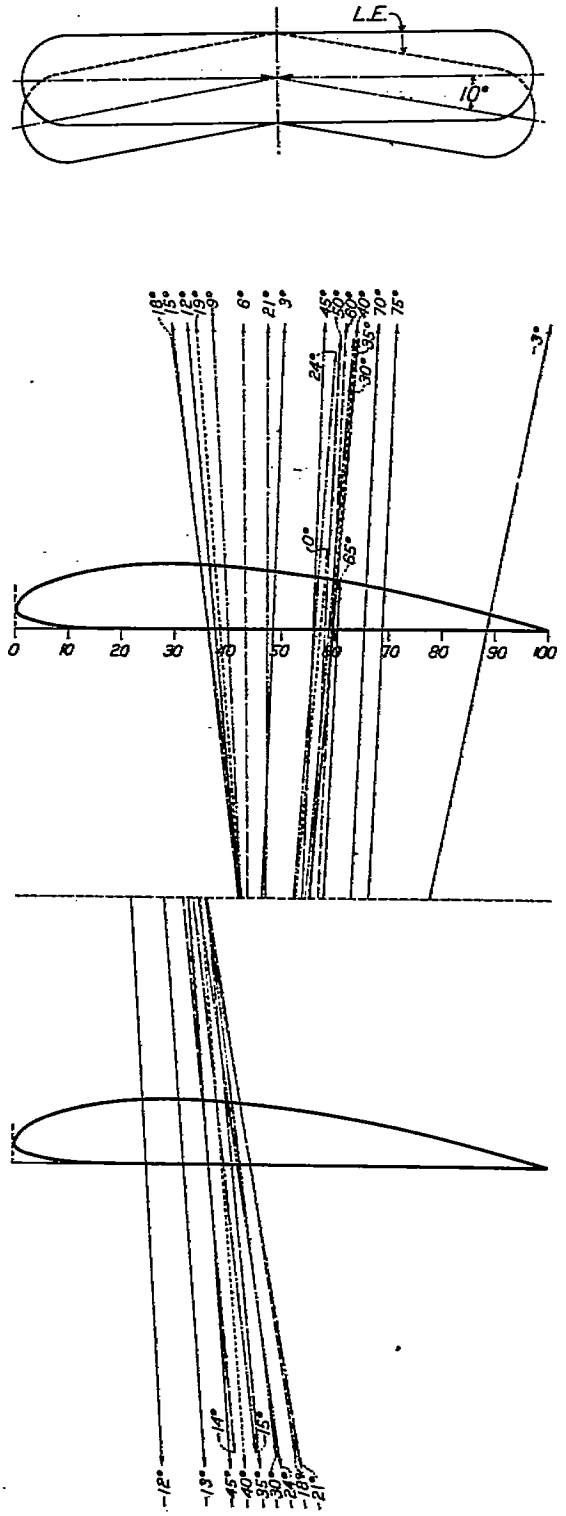

FIGURE 44.—Biplane vector diagram. Clark Y. Upper wing, straight. Lower wing, swept back. Circular tips. 5-inch chord. A. R. 6. Gap/chord=1. Decalage, 0°. Stagger, 0

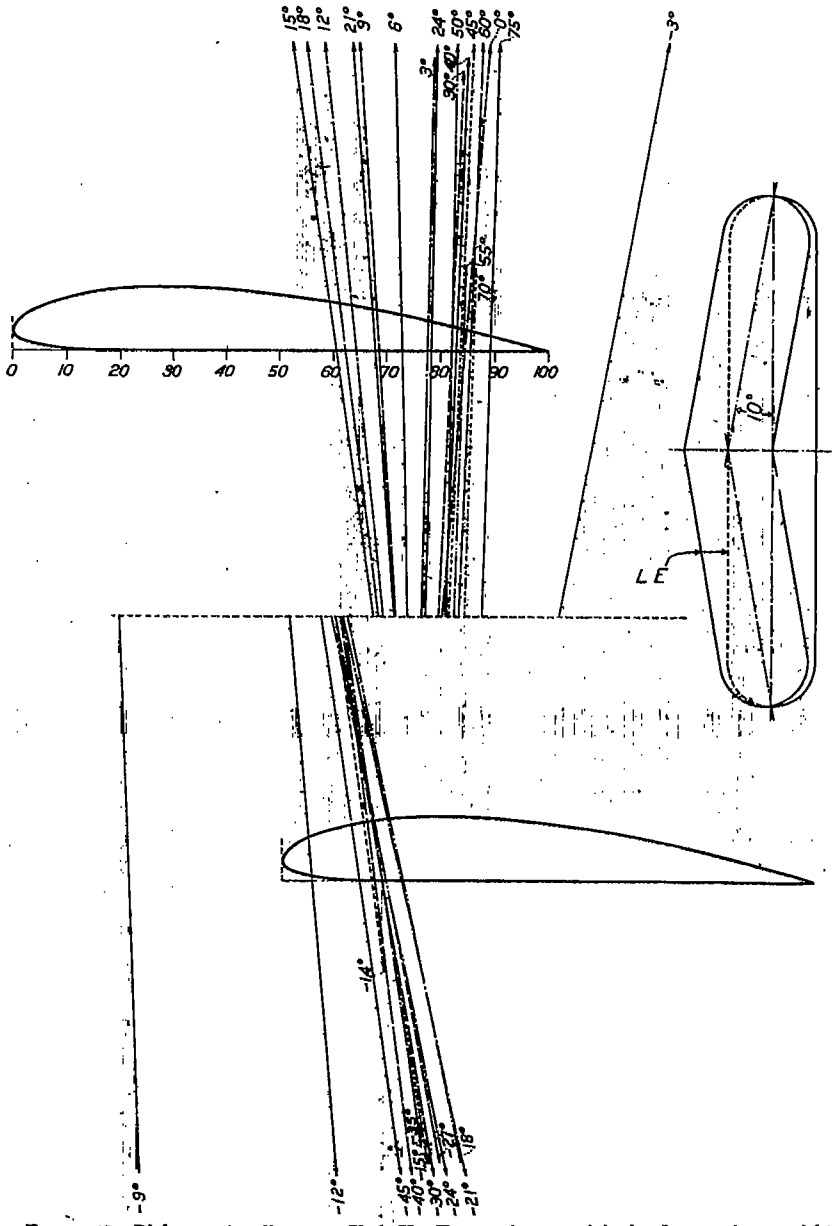

FIGURE 45.—Biplane vector diagram. Clark Y. Upper wing, swept back. Lower wing, straight. Circular tips. 5-inch chord. A. R. 6. Gap/chord=1. Decalage, 0°. Stagger, +50 per cent chord

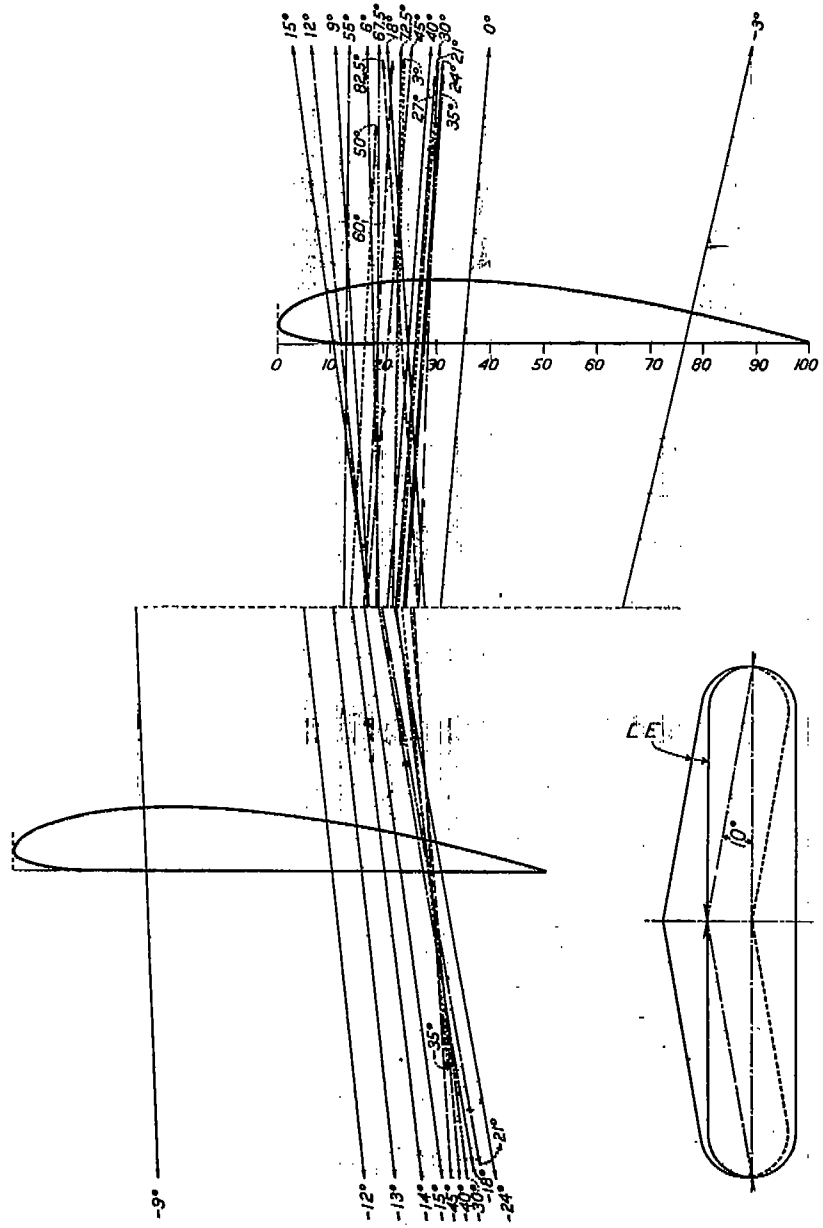

FIGURE 46.—Biplane vector diagram. Clark Y. Upper wing, straight. Lower wing, swept back. Circular tips. 5-inch chord. A. R. 6. Gap/chord=1. Decalage, 0°. Stagger, −50 per cent chord

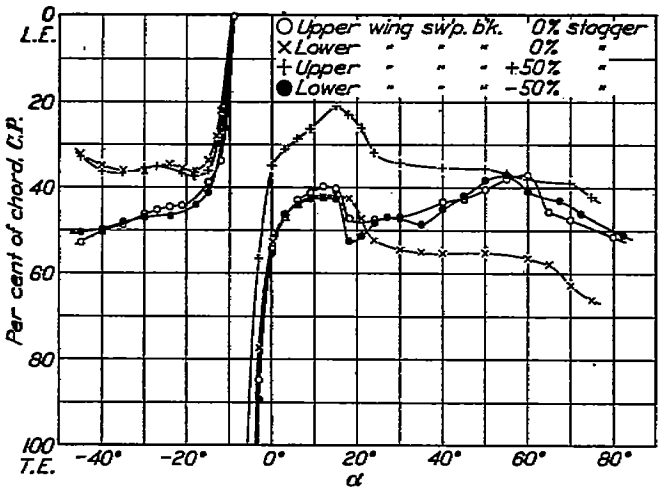

FIGURE 47.—Biplane wings. Sweep-back effect. Clark Y. Circular tips. 5-inch chord. A. R. 6. Gap/chord=1. Decalage, 0°

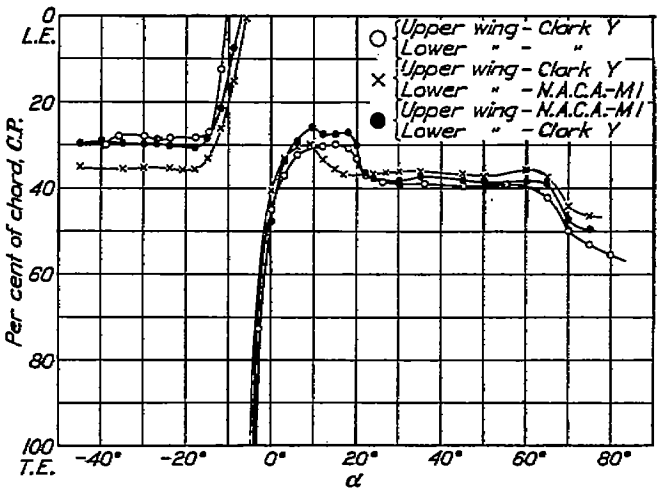

FIGURE 48.—Biplane wings. Profile effect. Clark Y. and N. A. C. A.-M1. Circular tips. 5-inch chord. A. R. 6. Gap/chord=1. Decalage, 0°. Stagger, 0

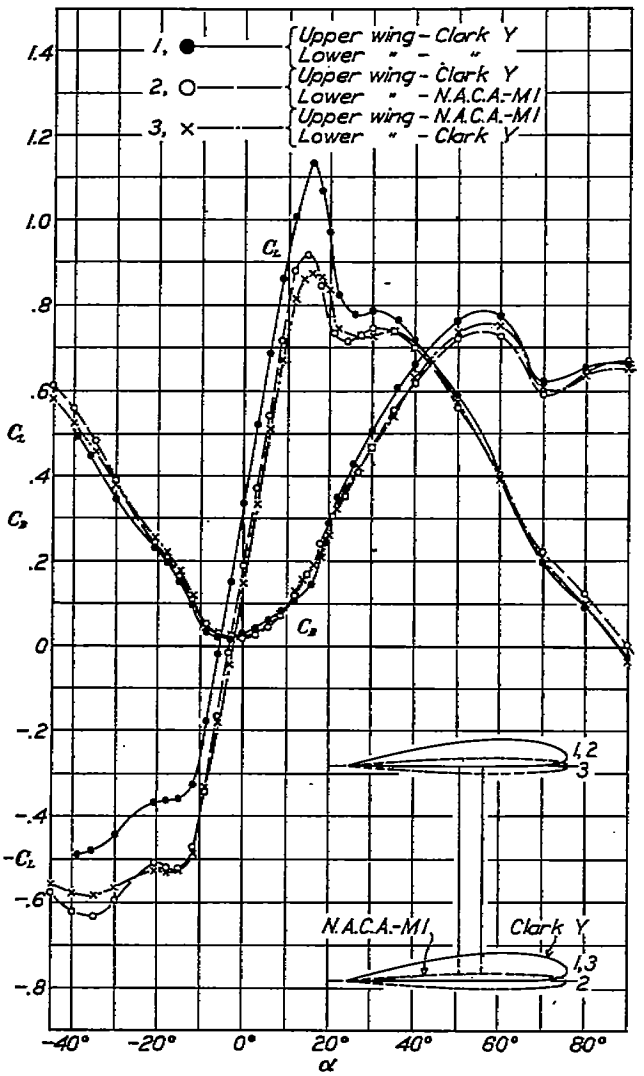

FIGURE 49.—Biplane wings. Profile effect. Clark Y. N. A. C. A.-M1. Circular tips. 5-inch chord. A. R. 6. Gap/chord=1. Decalage, 0°. Stagger, 0

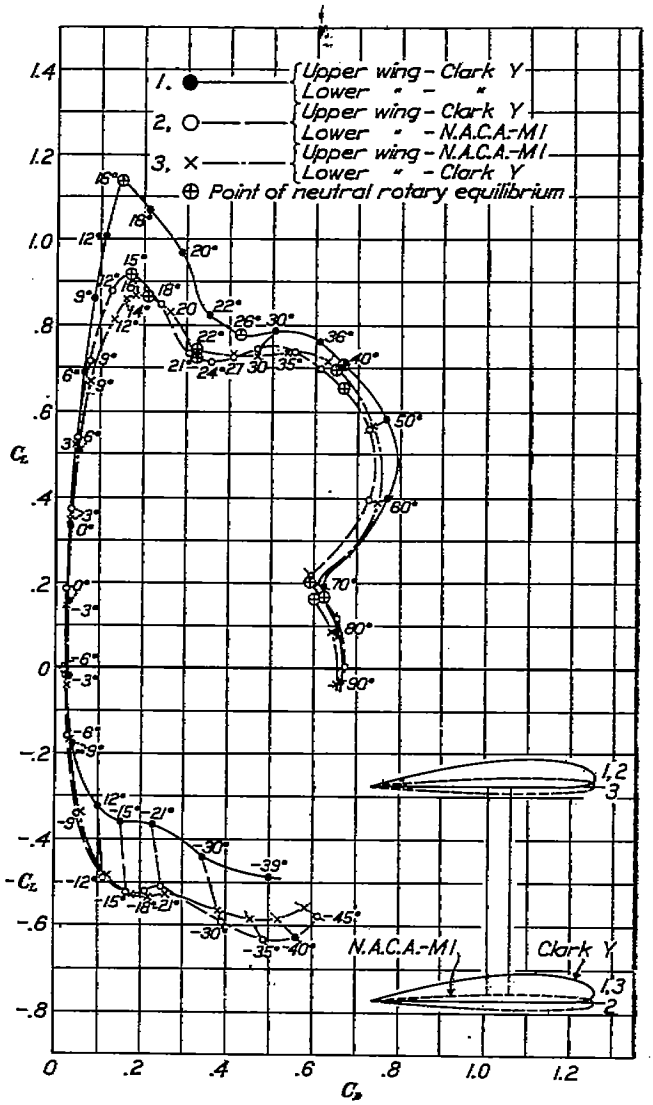

FIGURE 50.—Biplane wings. Profile effect. Polars. Clark Y. N. A. C. A.-M1. Circular tips. 5-inch chord. A. R. 6. Gap/chord=1. Decalage, 0°. Stagger, 0

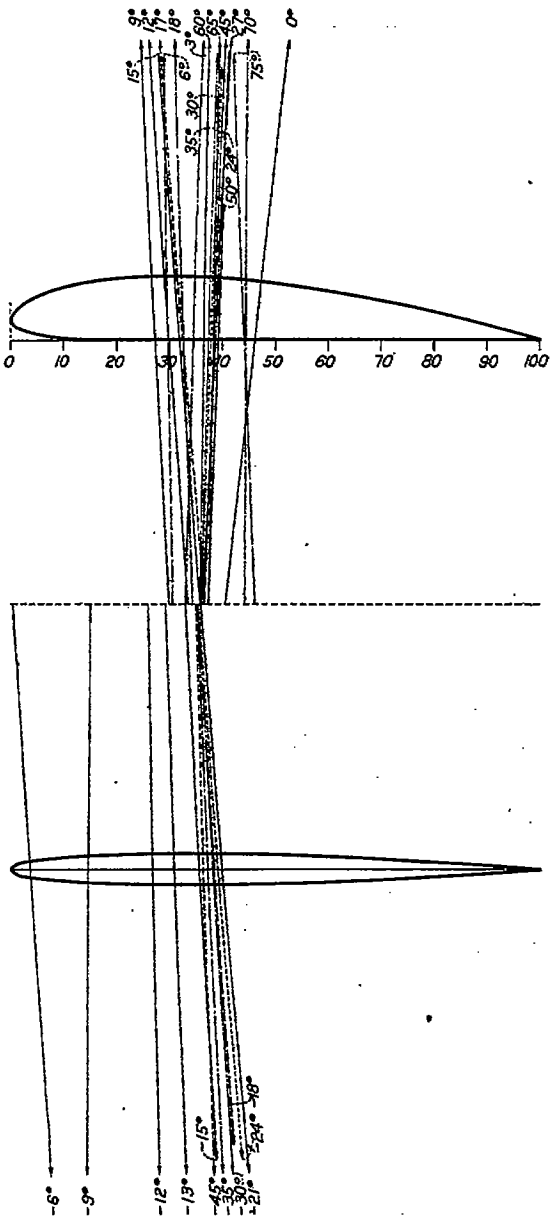

FIGURE 51.—Biplane vector diagram. Upper wing, Clark Y. Lower wing, N. A. C. A.-M1. Circular tips. 5-inch chord. A. R. 6. Gap/chord=1. Decalage, 0°. Stagger, 0

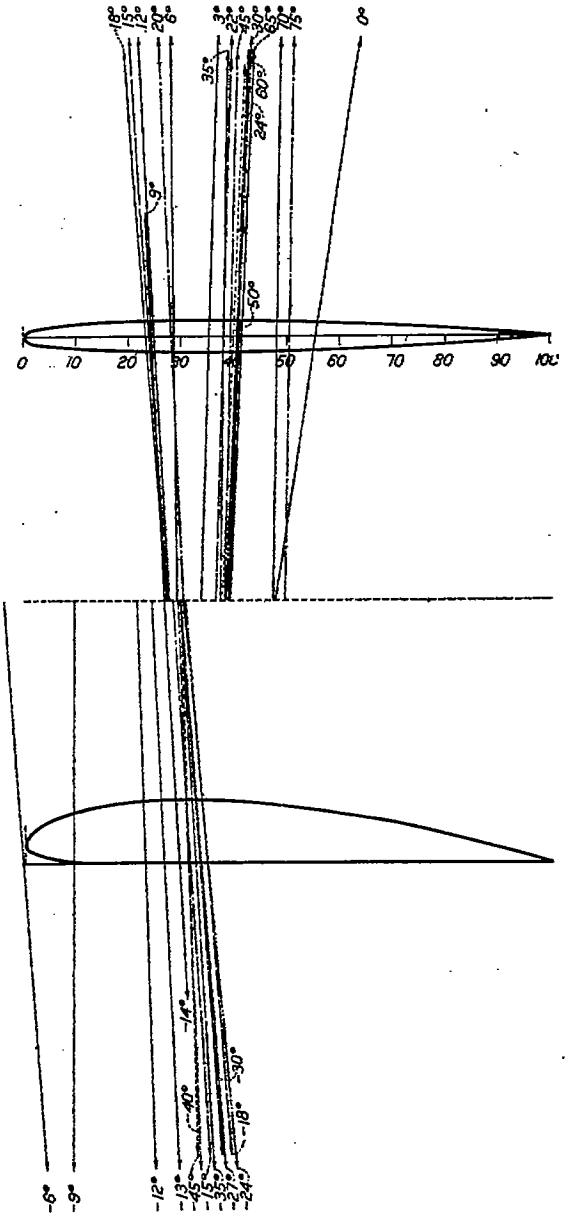

FIGURE 52.—Biplane vector diagram. Upper wing, N. A. C. A.-M1. Lower wing, Clark Y. Circular tips. 5-inch chord. A. R. 6. Gap/chord=1. Decalage, 0°. Stagger, 0

APPENDIX

By Thomas A. Harris

In the force tests described in the foregoing report, the dynamic pressure was maintained constant at the position of the "service Pitot." (Fig. 53.) This dynamic pressure q', is a certain fraction of the dynamic pressure q, at the position of the model (with model removed from the tunnel), several feet downstream with the honeycomb between it and the "service Pitot." (Fig. 53.) In order to determine the relation between q' and q, a Pitot-static survey was conducted at the position of the model, and the "service Pitot" was then calibrated against this survey.

Since this wind tunnel is of the closed throat test section type, if part of the test section is blocked by a model, the same amount of air must pass through the restricted area that formerly passed through the unobstructed section. With the model at small angles of attack, the blocked area is small, but at large angles the blocking causes the dynamic pressure q'', at the position of the model, to increase appreciably, while it does not affect the dynamic pressure q', at the "service Pitot." The variable dynamic pressure q'', is the value from which the absolute coefficients should be calculated. In the tests described in the foregoing report, however, the absolute coefficients C_D and C_L (uncorrected for blocking), were calculated from values of q. Since q is less than q'', these coefficients are higher than C_D' and C_L' (corrected for blocking).

TESTS

To determine the blocking correction, force tests were made on a series of rectangular "flat" plates, with 3, 4, 5, 6, and 7 inch chords, and of aspect ratio 6. The upstream surface of each plate was flat, while the downstream surface was pyramidal in form, beveled 15° from all edges. These flat plates were used instead of airfoils because they were more easily constructed, and answered the same purpose.

The force tests on these plates were made on the regular wire balance of the wind tunnel. (Reference 2.) Lift and drag data were obtained for angles of attack ranging from 20° to 90°, and the absolute coefficients (C_D and C_L) were then calculated. All tests were run at an average Reynolds Number of 153,000, the chord length being taken as the characteristic dimension.

RESULTS

The results of the force tests on the flat plates are given in Table XXIX, and as curves in Figures 57a and 58a. C_D was also plotted against the areas of the flat plates for the various angles of attack (Figure 54). These curves were extrapolated to zero area (as shown by the broken lines), to obtain C_D' the absolute free air coefficient.

From the curves (fig. 54) it can readily be seen that:

$$C_D' = KC_D \tag{1}$$

from which it follows that

$$K = \frac{C_D'}{C_D} \tag{2}$$

Values of K were calculated for the several plates at the various angles of attack by means of equation (2), and by data obtained from the curves. (Fig. 54.) It is apparent that K is a function of the area ratio (a/A), where a is the projected area of the model perpendicular to the air stream, and A is the cross-sectional area of the tunnel at the test section. Values of (a/A)

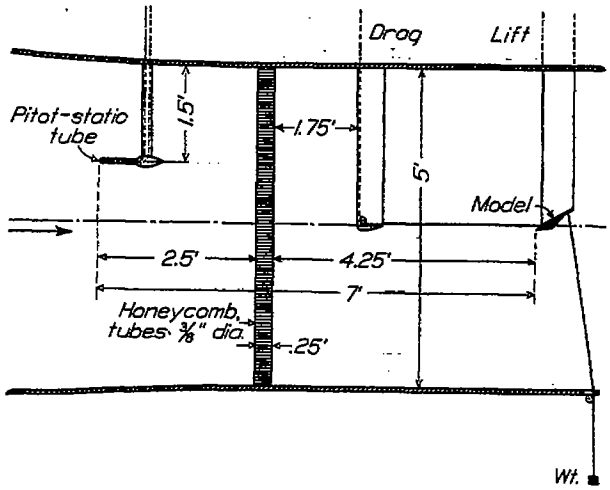

FIGURE 53.—Blocking tests. Wind tunnel set-up

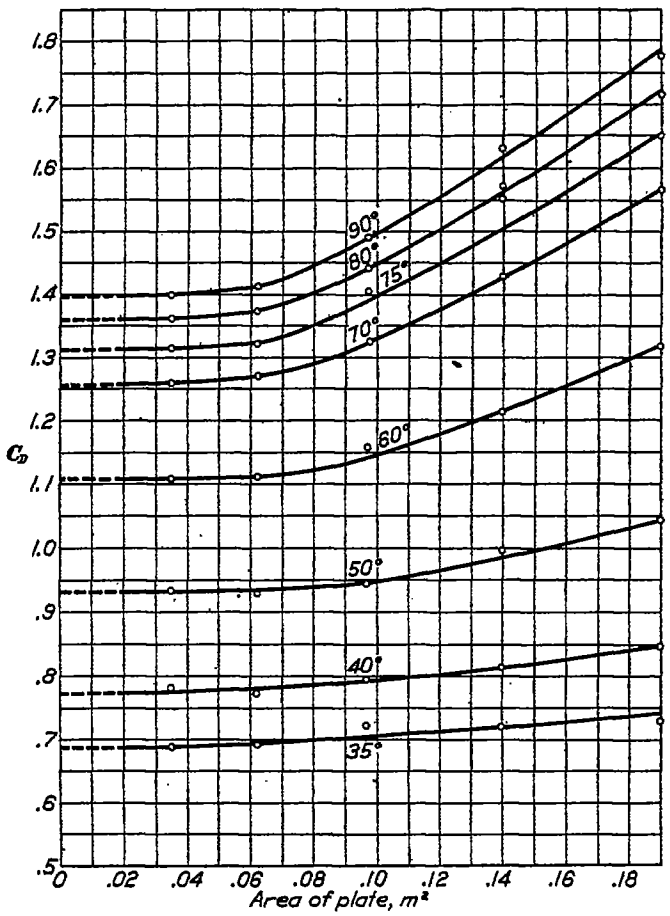

FIGURE 54.—Drag versus area of plate

with the corresponding values of K are given in Table XXVIII, and are plotted in logarithmic form in Figure 55. It was found that a straight line could be drawn through these points, with a maximum deviation of about 2 per cent.

From an analysis of this line it was found that:

$$K = 1 - 6.75\ (a/A)^{2.4} \tag{3}$$

This equation was plotted on regular cross-section paper (Figure 56) to be used in finding corrections for C_D and C_L for any value of area ratio up to about 0.08. The area ratios of the 7-inch chord flat plate exceeded this value and the curve of the equation would not pass through these points. A broken line is, however, faired through them.

As (a/A) increases, q'' also increases while q' is kept constant. Therefore the lift and drag are both affected and the same correction applies to each. C_D was used for determining the blocking correction because as the angle of attack increases, C_D increases, while C_L decreases,

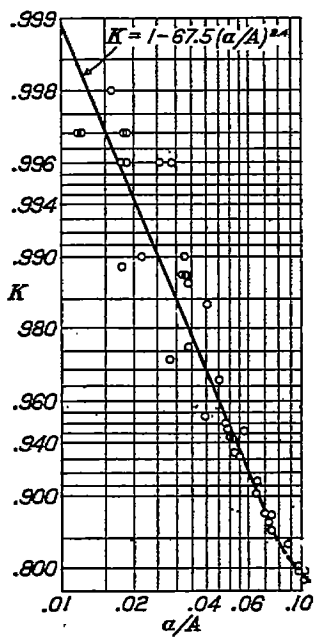

FIGURE 55.—Blocking correction versus area ratio (logarithmic)

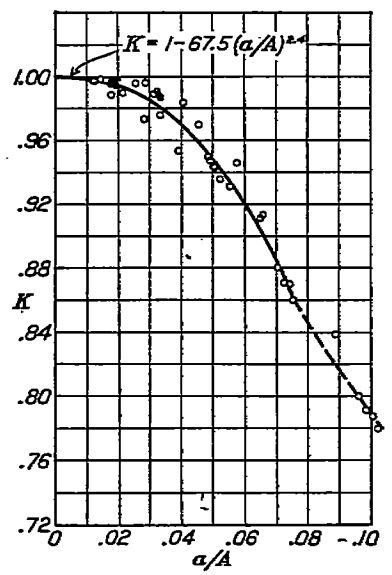

FIGURE 56.—Blocking correction versus area ratio

and for large angles of attack the experimental error becomes a larger percentage of the C_L results.

By use of equation (3) the flat plate data for chord lengths 3, 4, 5, and 6 inches were corrected. The values of C_D, C_L, C_D', and C_L' are given in Table XXIX, and are plotted in Figures 57 a and b, and 58 a and b, as absolute coefficients vs. angle of attack, and as polars. The corrected points are within the experimental error of the force test results for the flat plates. The limit of (a/A) for the flat plate tests was about 0.10. This value is safely beyond any value of (a/A) used in the series of wing model tests.

To verify formula (3), the correction was applied to the data obtained from force tests on two circular tipped Clark Y airfoils, of aspect ratio 8, with 3 and 5 inch chords. These data are given in Table XXX and are plotted in Figures 59 a and b, and 60 a and b, as absolute coefficients vs. angle of attack, and as polars. The corrected values of C_D and C_L for the airfoils are, in general, within 1 per cent of the faired curves, which is within the experimental error of the force tests.

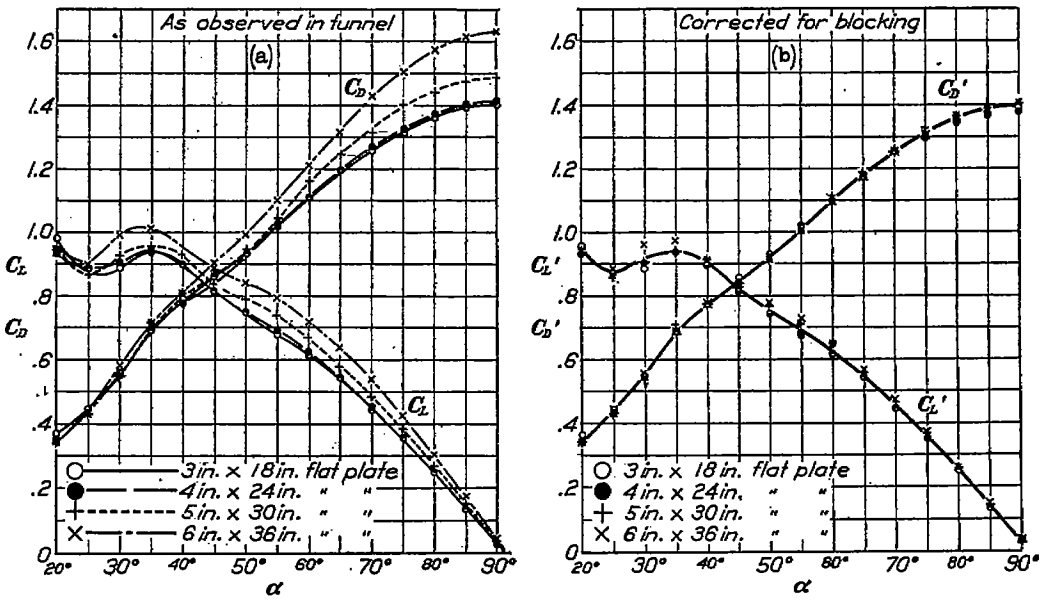

FIGURE 57.—Flat plates. A. R. 6

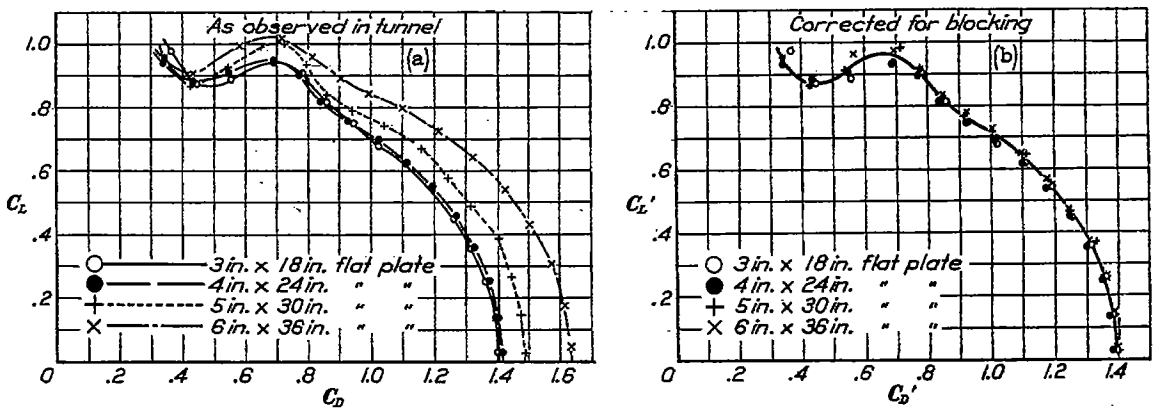

FIGURE 58.—Flat plates. A. R. 6. Polars

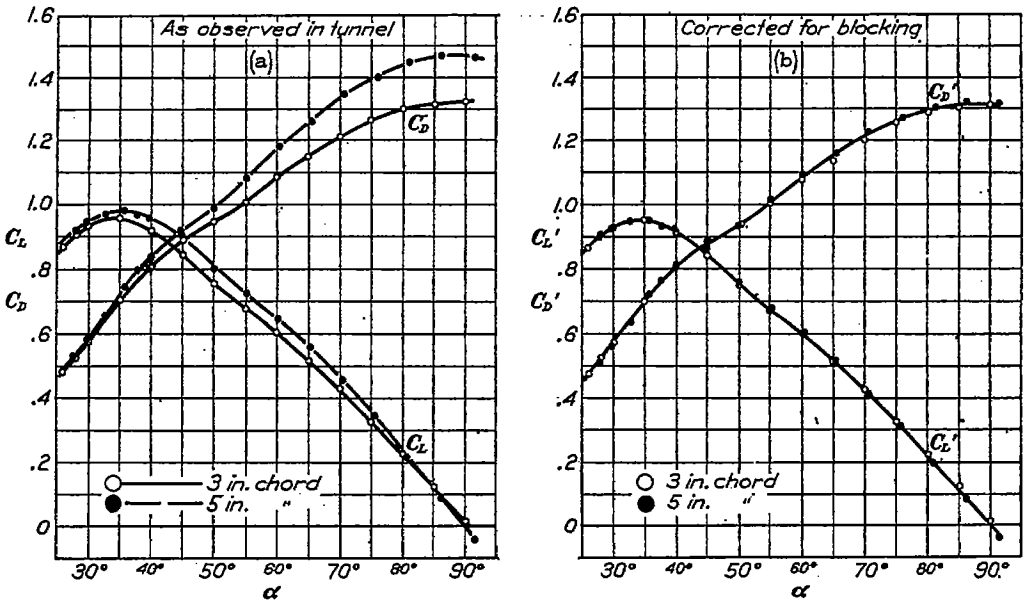

FIGURE 59.—Clark Y wings. A. R. 8

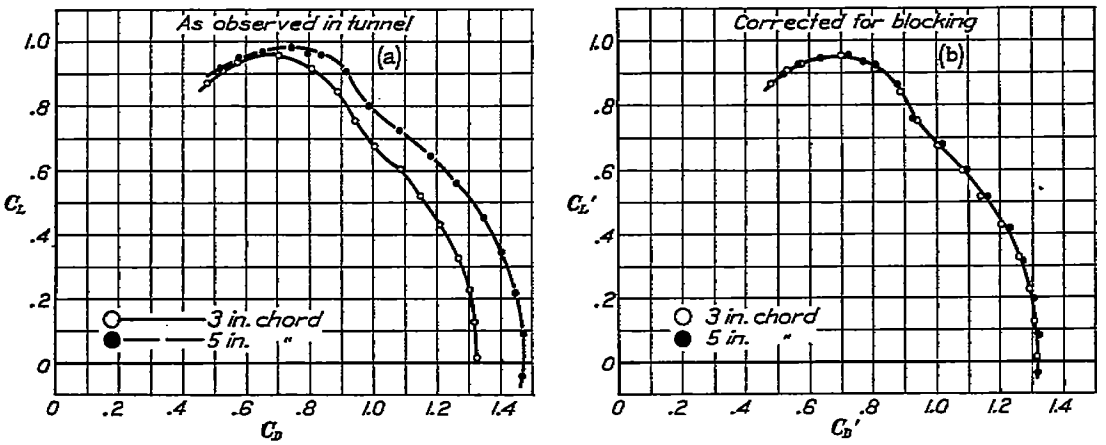

FIGURE 60.—Clark Y wings. A. R. 8. Polars

CONCLUSIONS

1. A blocking correction curve for monoplane test results has been obtained which applies to this wind tunnel for ratios of projected area of the model to cross-sectional area of the tunnel up to about 0.10.

2. Further research is necessary to obtain a similar correction for biplane test results at large angles of attack.

3. It is highly desirable that some means be devised for maintaining the dynamic pressure constant in the vicinity of the model, regardless of the change in angle of attack, above maximum lift.

TABLE III

CALCULATED PROBABLE RANGES OF ROTARY INSTABILITY

Model	Rotary instability								
	Normal spinning range			Flat spinning range			Inverted spinning range		
	α° limits		Range	α° limits		Range	α° limits		Range
	Lower	Upper		Lower	Upper		Lower	Upper	
Monoplane	*Degrees*	*Degrees*	*Degrees*	*Degrees*	*Degrees*	*Degrees*	*Degrees*	*Degrees*	*Degrees*
Rectangular tip	14.5	24.5	10.0	------	------	0	------	------	0
Negative rake tip	15.0	26.0	11.0	------	------	0	------	------	0
Circular tip A. R.=6	14.5	24.0	9.5	------	------	0	−13.0	−16.0	3.0
Circular tip A. R.=4	17.5	26.0	8.5	------	------	0	−15.5	−21.0	5.5
Circular tip A. R.=8	13.5	24.0	10.5	------	------	0	0	0	0
Flap 15° up	17.0	26.0	9.0	------	------	0	−11.0	−16.5	5.5
Flap 15° down	13.0	20.0	7.0	------	------	0	−12.5	−22.0	9.5
Flap 25° down	12.0	20.0	8.0	------	------	0	−18.0	−20.0	2.0
Flap 30° down	11.0	19.5	8.5	------	------	0	−32.0	−37.0	5.0
N. A. C. A. M-1 A. R.=6	12.0	14.5	2.5	------	------	0	−12.0	−14.5	2.5
Biplane									
Stagger −25%	15.0	24.0	9.0	33.5	60.0	26.5	------	------	0
Stagger 0%	16.0	26.0	10.0	40.0	74.0	34.0	------	------	0
Stagger +25%	16.0	24.0	8.0	55.0	90.0	35.0	------	------	0
Stagger +50%	15.0	24.0	9.0	62.0	------	------	------	------	0
Gap/chord 1.5	15.0	23.0	8.0	44.0	80.0	36.0	------	------	0
Gap/chord 0.5	17.0	24.0	7.0	30.0	64.0	34.0	------	------	0
Decalage +3°	14.5	24.0	9.5	37.0	75.0	38.0	------	------	0
Decalage −3°	18.0	29.0	11.0	42.0	73.0	31.0	------	------	0
Sweep back U. W. / Straight L. W. } 0% stagger[1]	16.0	24.5	8.5	35.0	62.5	27.5	------	------	0
Straight U. W. / Sweep back L. W. } 0% stagger[1]	16.0	23.5	7.5	50.0	------	------	−14.0	−17.0	3.0
Sweep back U. W. / Straight L. W. } +50% stagger[1]	16.0	27.0	11.0	55.0	------	------	−14.0	−17.0	3.0
Straight U. W. / Sweep back L. W. } −50% stagger[1]	16.0	24.5	8.5	35.0	67.5	32.5	------	------	0
Clark Y. U. W. / N. A. C. A.-M1 L. W. }	15.0	22.0	7.0	45.0	71.0	26.0	------	------	0
N. A. C. A. M-1 U. W. / Clark Y. L. W. }	18.0	22.0	4.0	42.0	73.0	31.0	------	------	0

[1] Stagger measured at midspan.

TABLE IV

FORCE TEST

Clark Y monoplane. 5-inch chord.
Aspect ratio=6. Rectangular tips.
q=19.86 kg/m²
Reynolds No.=149,000.

$\alpha°$	C_D	C_L	$\alpha°$	C_D	C_L
−45	0. 665	−0. 638	17	0. 218	1. 130
−42	. 618	−. 651	18	. 245	1. 080
−39	. 584	−. 654	19	. 286	. 885
−36	. 532	−. 659	20	. 321	. 844
−33	. 461	−. 610	22	. 362	. 805
−30	. 380	−. 542	24	. 397	. 805
−27	. 323	−. 493	26	. 441	. 812
−24	. 275	−. 467	28	. 485	. 844
−21	. 232	−. 426	30	. 552	. 870
−18	. 186	−. 392	32	. 600	. 880
−15	. 153	−. 384	34	. 630	. 886
−14	. 139	−. 378	37	. 693	. 880
−13	. 126	−. 371	40	. 749	. 842
−12	. 110	−. 371	45	. 811	. 780
−9	. 037	−. 301	50	. 894	. 733
−6	. 019	−. 018	55	. 983	. 681
−3	. 018	+. 188	60	1. 065	. 614
0	. 022	. 412	65	1. 170	. 525
+3	. 035	. 630	70	1. 260	. 431
6	. 052	. 844	75	1. 310	. 322
9	. 081	1. 030	80	1. 345	. 203
12	. 105	1. 180	85	1. 357	. 078
15	. 156	1. 220	90	1. 367	. 000
16	. 198	1. 160			

TABLE V

FORCE TEST

Clark Y monoplane. 5-inch chord.
Aspect ratio=6. Negative rake tips.
q=19.92 kg/m²
Reynolds No.=149,000.

$\alpha°$	C_D	C_L	$\alpha°$	C_D	C_L
−45	0. 643	−0. 589	16	0. 159	1. 184
−42	. 574	−. 593	17	. 216	1. 118
−39	. 531	−. 604	18	. 254	1. 067
−36	. 496	−. 628	19	. 306	. 893
−33	. 436	−. 577	20	. 319	. 838
−30	. 362	−. 526	22	. 362	. 800
−27	. 311	−. 479	24	. 391	. 769
−24	. 265	−. 441	26	. 428	. 775
−21	. 227	−. 423	28	. 477	. 794
−18	. 195	−. 429	30	. 531	. 833
−15	. 157	−. 426	33	. 615	. 857
−14	. 145	−. 421	36	. 658	. 818
−13	. 130	−. 415	40	. 716	. 796
−12	. 110	−. 403	45	. 808	. 753
−9	. 032	−. 254	50	. 908	. 715
−6	. 018	−. 047	55	1. 005	. 670
−3	. 019	+. 139	60	1. 092	. 597
0	. 023	. 366	65	1. 172	. 515
+3	. 035	. 566	70	1. 237	. 422
6	. 051	. 785	75	1. 283	. 322
9	. 073	. 988	80	1. 315	. 214
12	. 099	1. 130	85	1. 332	+. 091
15	. 142	1. 181	90	1. 340	−. 018

TABLE VI

FORCE TEST

Clark Y monoplane. 5-inch chord.
Aspect ratio=6. Circular tips.
q=19.90 kg/m²
Reynolds No.=151,000.

$\alpha°$	C_D	C_L	$\alpha°$	C_D	C_L
−45	0. 646	−0. 626	17	0. 188	1. 130
−42	. 611	−. 648	18	. 246	1. 053
−39	. 564	−. 639	19	. 291	. 985
−36	. 511	−. 637	20	. 322	. 869
−33	. 434	−. 593	22	. 356	. 803
−30	. 369	−. 522	24	. 376	. 794
−27	. 307	−. 466	26	. 426	. 781
−24	. 262	−. 438	28	. 482	. 823
−21	. 224	−. 402	30	. 552	. 874
−18	. 187	−. 383	33	. 619	. 906
−15	. 153	−. 391	36	. 688	. 872
−14	. 141	−. 402	38	. 711	. 841
−13	. 125	−. 408	40	. 733	. 815
−12	. 108	−. 397	45	. 808	. 769
−9	. 032	−. 240	50	. 904	. 722
−6	. 021	−. 019	55	1. 000	. 675
−3	. 017	+. 176	60	1. 090	. 608
0	. 021	. 398	65	1. 170	. 524
+3	. 034	. 614	70	1. 240	. 435
6	. 050	. 813	75	1. 290	. 321
9	. 073	1. 012	80	1. 330	. 215
12	. 101	1. 148	85	1. 360	+. 098
15	. 149	1. 172	90	1. 360	−. 017
16	. 169	1. 154			

TABLE VII

FORCE TEST

Clark Y monoplane. 5-inch chord.
Aspect ratio=4. Circular tips.
q=19.94 kg/m²
Reynolds No.=151,000.

$\alpha°$	C_D	C_L	$\alpha°$	C_D	C_L
−45	0. 576	−0. 549	16	0. 166	1. 157
−42	. 523	−. 541	17	. 189	1. 157
−39	. 475	−. 523	18	. 203	1. 149
−36	. 427	−. 506	19	. 222	1. 117
−33	. 381	−. 479	20	. 287	1. 000
−30	. 336	−. 458	22	. 345	. 852
−27	. 288	−. 427	24	. 373	. 769
−24	. 248	−. 392	26	. 396	. 743
−21	. 214	−. 371	28	. 426	. 743
−18	. 202	−. 410	30	. 458	. 735
−15	. 160	−. 449	33	. 509	. 735
−14	. 142	−. 445	36	. 561	. 739
−13	. 123	−. 422	40	. 642	. 733
−12	. 099	−. 384	45	. 744	. 712
−9	. 031	−. 204	50	. 846	. 673
−6	. 019	−. 048	55	. 933	. 611
−3	. 017	+. 135	60	1. 020	. 551
0	. 021	. 328	65	1. 096	. 473
+3	. 037	. 513	70	1. 155	. 378
6	. 056	. 696	75	1. 201	. 279
9	. 082	. 870	80	1. 240	. 161
12	. 112	1. 035	85	1. 249	+. 061
15	. 144	1. 142	90	1. 246	−. 057

TABLE VIII

FORCE TEST

Clark Y monoplane. 5-inch chord.
Aspect ratio=8. Circular tips.
q=19.94 kg/m²
Reynolds No. =153,000.

$\alpha°$	C_D	C_L	$\alpha°$	C_D	C_L
−45	0.750	−0.740	17	0.205	1.098
−42	.681	−.752	18	.245	1.050
−39	.620	−.737	19	.300	.935
−36	.558	−.719	20	.321	.866
−33	.487	−.678	22	.365	.840
−30	.414	−.616	24	.400	.816
−27	.339	−.542	26	.457	.875
−24	.287	−.491	28	.528	.914
−21	.238	−.448	30	.578	.946
−18	.195	−.407	33	.654	.968
−15	.155	−.394	36	.742	.980
−14	.145	−.400	38	.795	.965
−13	.130	−.405	40	.838	.959
−12	.114	−.405	45	.916	.906
−9	.032	−.269	50	.986	.800
−6	.018	−.029	55	1.081	.723
−3	.017	+.171	60	1.180	.646
0	.019	.420	65	1.260	.560
+3	.028	.655	70	1.348	.453
6	.041	.883	75	1.400	.344
9	.061	1.075	80	1.446	.216
12	.086	1.192	85	1.470	+.089
15	.148	1.137	90	1.465	−.043
16	.172	1.128			

TABLE IX

FORCE TEST

Clark Y monoplane. 5-inch chord.
Aspect ratio=6. Circular tips.
Flap 20 per cent chord. 15° up.
q=19.87 kg/m²
Reynolds No.=151,000.

$\alpha°$	C_D	C_L	$\alpha°$	C_D	C_L
−44	0.738	−0.716	16	0.084	0.854
−41	.706	−.759	17	.101	.866
−38	.672	−.784	18	.118	.859
−35	.627	−.815	19	.164	.782
−32	.574	−.824	20	.187	.742
−29	.501	−.778	22	.252	.605
−26	.422	−.736	24	.284	.555
−23	.355	−.672	26	.305	.524
−20	.301	−.629	28	.336	.538
−17	.260	−.615	30	.369	.568
−14	.221	−.646	33	.450	.622
−13	.208	−.660	36	.525	.658
−12	.193	−.677	40	.617	.679
−11	.174	−.694	45	.686	.631
−8	.110	−.666	50	.756	.606
−5	.045	−.497	55	.842	.578
−3	.035	−.364	60	.939	.533
0	.028	−.182	65	1.033	.485
+3	.027	+.132	70	1.108	.413
6	.029	.345	75	1.171	.326
9	.041	.549	80	1.228	.242
12	.056	.723	85	1.257	.138
15	.072	.835	90	1.265	.037

TABLE X

FORCE TEST

Clark Y monoplane. 5-inch chord.
Aspect ratio=6. Circular tips.
Flap 20% chord. 15° down.
q=19.86 kg/m²
Reynolds No.=153,000.

$\alpha°$	C_D	C_L	$\alpha°$	C_D	C_L
−44	0.520	−0.427	16	0.288	1.280
−41	.471	−.385	17	.321	1.218
−38	.418	−.354	18	.343	1.150
−35	.366	−.320	19	.389	.977
−32	.317	−.267	20	.407	.959
−29	.270	−.216	22	.446	.954
−26	.234	−.197	24	.491	.965
−23	.206	−.171	26	.554	.993
−20	.187	−.194	28	.616	1.032
−17	.170	−.258	30	.666	1.032
−14	.142	−.295	33	.718	.988
−13	.132	−.317	36	.761	.932
−12	.117	−.329	40	.823	.855
−11	.101	−.302	45	.912	.793
−8	.039	+.076	50	.998	.732
−5	.044	.323	55	1.082	.670
−3	.053	.488	60	1.169	.580
0	.067	.783	65	1.231	.476
+3	.081	.977	70	1.289	.383
6	.106	1.136	75	1.320	.273
9	.131	1.305	80	1.336	.146
12	.168	1.400	85	1.350	+.031
15	.235	1.370	90	1.334	−.090

TABLE XI

FORCE TEST

Clark Y monoplane. 5-inch chord.
Aspect ratio=6. Circular tips.
Flap 20% chord. 25° down.
q=19.85 kg/m²
Reynolds No.=153,000.

$\alpha°$	C_D	C_L	$\alpha°$	C_D	C_L
−44	0.448	−0.266	17	0.371	1.160
−41	.404	−.268	18	.422	.986
−38	.383	−.282	19	.446	.973
−35	.378	−.352	20	.466	.955
−32	.357	−.391	22	.529	.966
−29	.312	−.394	24	.586	1.000
−26	.279	−.391	26	.649	1.005
−23	.243	−.386	28	.695	.995
−20	.211	−.386	30	.734	.977
−17	.178	−.405	33	.773	.950
−14	.139	−.358	36	.800	.921
−13	.121	−.316	38	.829	.899
−12	.107	−.260	40	.845	.874
−11	.083	−.120	45	.945	.800
−8	.056	+.299	50	1.042	.727
−5	.066	.515	55	1.122	.655
−3	.078	.664	60	1.183	.565
0	.091	.855	65	1.245	.461
+3	.111	1.018	70	1.289	.360
6	.137	1.190	75	1.341	.236
9	.166	1.396	80	1.352	+.112
12	.212	1.450	85	1.342	−.008
15	.320	1.264	90	1.329	−.129
16	.354	1.190			

TABLE XII

FORCE TEST

Clark, Y monoplane. 5-inch chord.
Aspect ratio=6. Circular tips.
Flap 20% chord. 30° down.
q=19.85 kg/m²
Reynolds No.=152,000.

$\alpha°$	C_D	C_L	$\alpha°$	C_D	C_L
−44	0.500	−0.348	16	0.384	1.301
−41	.471	−.362	17	.425	1.095
−38	.450	−.376	18	.450	1.049
−35	.411	−.416	19	.475	1.040
−32	.394	−.466	20	.496	1.022
−29	.342	−.455	22	.548	1.049
−26	.296	−.429	24	.614	1.090
−23	.255	−.421	26	.673	1.096
−20	.223	−.426	28	.713	1.079
−17	.190	−.432	30	.741	1.057
−14	.142	−.381	33	.793	.983
−13	.130	−.328	36	.817	.916
−12	.113	−.278	40	.884	.853
−11	.101	−.177	45	.979	.795
−8	.067	+.345	50	1.063	.721
−5	.075	.553	55	1.139	.651
−3	.092	.680	60	1.210	.545
0	.110	.919	65	1.262	.444
+3	.129	1.112	70	1.310	.329
6	.159	1.307	75	1.330	.213
9	.189	1.483	80	1.351	+.093
12	.237	1.498	85	1.338	−.031
15	.346	1.377	90	1.313	−.124

TABLE XIII

FORCE TEST

N. A. C. A.–M1 monoplane. 5-inch chord.
Aspect ratio=6. Circular tips.
q=19.95 kg/m²
Reynolds No.=153,000.

	$\alpha°$	C_D	C_L	$\alpha°$	C_D	C_L
Symmetry assumed for negative angles	−42	0.727	−0.820	16	0.212	0.699
	−36	.636	−.871	17	.229	.702
	−33	.570	−.863	18	.245	.705
	−30	.485	−.820	19	.260	.699
	−28	.428	−.774	20	.271	.693
	−26	.374	−.729	22	.300	.702
	−24	.332	−.713	24	.332	.713
	−22	.300	−.702	26	.374	.729
	−20	.271	−.693	28	.428	.774
	−19	.260	−.699	30	.485	.820
	−18	.245	−.705	33	.570	.863
	−17	.229	−.702	36	.636	.871
	−16	.212	−.699	42	.727	.820
	−15	.196	−.704	45	.770	.765
	−12	.149	−.721	50	.854	.716
	−9	.074	−.610	55	.950	.675
	−6	.032	−.398	60	1.049	.622
	−3	.015	−.189	65	1.129	.551
	0	.012	−.003	70	1.218	.474
	+3	.015	+.189	75	1.289	.371
	6	.032	.398	80	1.340	.273
	9	.074	.610	85	1.378	.156
	12	.149	.721	90	1.367	.045
	15	.196	.704			

TABLE XIV

FORCE TEST

Clark Y biplane. 5-inch chord.
Aspect ratio=6. Circular tips.
Stagger=−25 per cent chord. G/c=1.0
Decalage=0°. q=19.92 kg/m²
Reynolds No.=152,000.

$\alpha°$	C_D	C_L	$\alpha°$	C_D	C_L
−40	0.542	−0.542	15	0.138	1.090
−36	.470	−.529	16	.164	1.075
−33	.417	−.509	18	.211	1.006
−30	.367	−.484	20	.288	.879
−27	.318	−.453	22	.336	.771
−24	.272	−.425	24	.369	.743
−21	.231	−.398	26	.433	.742
−18	.199	−.395	28	.470	.745
−15	.157	−.381	30	.484	.757
−14	.142	−.372	35	.581	.740
−13	.123	−.357	40	.615	.655
−12	.103	−.338	45	.610	.550
−9	.036	−.184	50	.603	.450
−6	.024	−.022	55	.561	.350
−3	.023	+.150	60	.527	.286
0	.028	.333	65	.555	.247
+3	.040	.514	70	.606	.199
6	.058	.695	75	.633	.145
9	.079	.860	80	.652	.086
12	.106	.999	85	.658	+.029
14	.128	1.083	90	.657	−.035

TABLE XV

FORCE TEST

Clark Y biplane. 5-inch chord.
Aspect ratio=6. Circular tips.
Stagger=0. G/c=1.0.
Decalage=0°. q=19.94 kg/m²
Reynolds No.=151,000.

$\alpha°$	C_D	C_L	$\alpha°$	C_D	C_L
−39	0.495	−0.489	18	0.210	1.068
−36	.449	−.482	19	.249	1.027
−33	.400	−.465	20	.286	.971
−30	.343	−.441	22	.352	.821
−27	.302	−.409	24	.393	.801
−24	.270	−.384	26	.424	.776
−21	.226	−.369	28	.463	.777
−18	.196	−.362	30	.505	.786
−15	.152	−.359	33	.559	.785
−14	.137	−.356	36	.610	.765
−13	.116	−.341	38	.633	.736
−12	.098	−.324	40	.664	.709
−9	.035	−.176	45	.726	.657
−6	.025	−.017	50	.764	.584
−3	.025	+.154	55	.791	.521
0	.029	.335	60	.773	.400
+3	.042	.523	65	.704	.287
6	.059	.689	70	.624	.193
9	.082	.863	75	.634	.145
12	.108	1.009	80	.660	.090
15	.135	1.103	85	.668	+.031
16	.145	1.135	90	.664	−.032
17	.163	1.121			

TABLE XVI

FORCE TEST

Clark Y biplane. 5-inch chord.
Aspect ratio=6. Circular tips.
Stagger=+25 per cent chord. G/c=1.0.
Decalage=0°. q=19.88 kg/m²
Reynolds No.=151,000.

$\alpha°$	C_D	C_L	$\alpha°$	C_D	C_L
−45	0.509	−0.402	16	0.157	1.156
−42	.500	−.440	17	.172	1.153
−39	.474	−.460	18	.219	1.091
−36	.424	−.454	19	.238	1.078
−33	.369	−.428	20	.256	1.048
−30	.325	−.404	22	.335	.934
−27	.284	−.377	24	.411	.875
−24	.244	−.348	26	.456	.857
−21	.215	−.338	28	.491	.829
−18	.180	−.336	30	.526	.837
−15	.145	−.336	35	.640	.842
−14	.124	−.337	40	.735	.809
−13	.112	−.329	45	.819	.764
−12	.091	−.310	50	.890	.689
−9	.031	−.157	55	.962	.616
−6	.021	+.027	60	.995	.525
−3	.023	.167	65	.999	.419
0	.028	.356	70	.958	.306
+3	.047	.542	75	.877	.190
6	.059	.725	80	.736	.086
9	.082	.862	85	.686	+.025
12	.109	1.050	90	.677	−.031
15	.143	1.153			

TABLE XVII

FORCE TEST

Clark Y biplane. 5-inch chord.
Aspect ratio=6. Circular tips.
Stagger=+50 per cent chord. G/c=1.0.
Decalage=0°. q=19.94 kg/m²
Reynolds No.=153,000.

$\alpha°$	C_D	C_L	$\alpha°$	C_D	C_L
−42	0.408	−0.377	15	0.169	1.156
−39	.394	−.413	16	.215	1.104
−36	.365	−.420	17	.234	1.094
−33	.325	−.404	18	.250	1.076
−30	.285	−.380	20	.304	1.008
−27	.252	−.355	22	.372	.947
−24	.219	−.341	24	.458	.914
−21	.188	−.328	26	.495	.879
−18	.156	−.327	28	.527	.857
−17	.141	−.330	30	.571	.862
−16	.136	−.331	35	.692	.865
−15	.126	−.327	40	.786	.841
−12	.071	−.299	45	.882	.791
−9	.033	−.134	50	.966	.737
−6	.021	+.039	55	1.048	.670
−3	.019	.220	60	1.122	.586
0	.027	.420	65	1.165	.477
+3	.047	.608	70	1.176	.364
6	.068	.790	75	1.146	.247
9	.094	.936	80	1.087	.158
12	.125	1.104	85	1.007	+.052
13	.138	1.131	90	.846	−.035
14	.155	1.150			

TABLE XVIII

FORCE TEST

Clark Y biplane. 5-inch chord.
Aspect ratio=6. Circular tips.
Stagger=0. G/c=1.5.
Decalage=0°. q=19.94 kg/m²
Reynolds No.=152,000.

$\alpha°$	C_D	C_L	$\alpha°$	C_D	C_L
−45	0.651	−0.582	13	0.122	1.106
−42	.586	−.574	14	.135	1.130
−39	.523	−.551	15	.149	1.135
−36	.467	−.529	16	.167	1.116
−33	.407	−.504	17	.184	1.107
−30	.351	−.473	18	.243	1.044
−27	.303	−.430	21	.342	.832
−24	.259	−.400	24	.403	.778
−21	.219	−.377	27	.460	.790
−18	.184	−.362	30	.516	.792
−15	.147	−.361	35	.636	.818
−14	.133	−.359	40	.741	.831
−13	.110	−.354	45	.826	.764
−12	.097	−.338	50	.879	.684
−9	.032	−.212	55	.924	.596
−6	.024	−.022	60	.930	.488
−3	.024	+.217	65	.866	.346
0	.030	.370	70	.741	.218
+3	.044	.559	75	.609	.134
6	.063	.750	80	.597	.089
9	.088	.924	85	.628	+.038
12	.116	1.073	90	.624	−.021

TABLE XIX

FORCE TEST

Clark Y biplane. 5-inch chord.
Aspect ratio=6. Circular tips.
Stagger=0. G/c=0.5.
Decalage=0°. q=19.95 kg/m²
Reynolds No.=153,000.

$\alpha°$	C_D	C_L	$\alpha°$	C_D	C_L
−45	0.456	−0.345	16	0.135	1.004
−42	.435	−.363	17	.153	1.010
−39	.413	−.366	18	.172	.999
−36	.393	−.408	19	.199	.971
−33	.367	−.422	20	.221	.951
−30	.328	−.410	22	.273	.851
−27	.277	−.390	24	.330	.811
−24	.236	−.370	26	.386	.811
−21	.194	−.353	28	.443	.802
−18	.157	−.342	30	.483	.794
−15	.113	−.311	35	.528	.688
−14	.099	−.304	40	.548	.587
−13	.085	−.289	45	.582	.516
−12	.069	−.263	50	.604	.453
−9	.031	−.136	55	.610	.379
−6	.024	+.003	60	.583	.303
−3	.024	.148	65	.594	.259
0	.029	.303	70	.629	.209
+3	.040	.460	75	.654	.156
6	.055	.610	80	.673	.102
9	.075	.760	85	.676	.049
12	.099	.903	90	.679	.020
15	.124	.995			

TABLE XX

FORCE TEST

Clark Y biplane. 5-inch chord.
Aspect ratio=6. Circular tips.
Stagger=0. G/c=1.0.
Decalage=+3°. q=19.94 kg/m²
Reynolds No.=153,000.

$\alpha°$	C_D	C_L	$\alpha°$	C_D	C_L
−45	0.547	−0.463	14	0.142	1.096
−40	.474	−.472	15	.177	1.082
−35	.398	−.446	18	.287	.926
−30	.319	−.402	21	.365	.823
−27	.276	−.380	24	.417	.766
−24	.240	−.363	27	.475	.763
−21	.202	−.356	30	.530	.776
−18	.167	−.345	35	.626	.754
−15	.122	−.335	40	.690	.692
−14	.102	−.315	45	.746	.630
−13	.079	−.282	50	.786	.555
−12	.062	−.244	55	.800	.458
−9	.028	−.067	60	.780	.357
−6	.026	+.054	65	.701	.241
−3	.027	.233	70	.629	.169
0	.036	.405	75	.638	.107
+3	.050	.594	80	.660	+.053
6	.071	.767	85	.664	−.013
9	.095	.920	90	.652	−.074
12	0.122	1.051			

TABLE XXI

FORCE TEST

Clark Y biplane. 5-inch chord.
Aspect ratio=6. Circular tips.
Stagger=0. G/c=1.0.
Decalage=−3.° q=20.03 kg/m²
Reynolds No.=154,000.

$\alpha°$	C_D	C_L	$\alpha°$	C_D	C_L
−45	0.574	−0.485	16	0.136	1.077
−40	.506	−.496	17	.150	1.096
−35	.440	−.479	18	.164	1.100
−30	.361	−.449	19	.177	1.089
−27	.314	−.424	20	.199	1.002
−24	.271	−.390	21	.248	.936
−21	.233	−.378	24	.352	.847
−18	.199	−.375	27	.422	.787
−15	.158	−.365	30	.464	.772
−14	.143	−.345	35	.562	.775
−13	.125	−.323	40	.630	.721
−12	.106	−.302	45	.693	.669
−9	.067	−.212	50	.735	.603
−6	.029	−.059	55	.756	.521
−3	.024	+.072	60	.745	.426
0	.026	.252	65	.692	.318
+3	.036	.437	70	.595	.236
6	.051	.613	75	.606	.185
9	.072	.782	80	.642	.126
12	.096	.937	85	.660	.067
15	.124	1.054	90	.658	.006

TABLE XXII

FORCE TEST

Clark Y biplane. 5-inch chord.
Upper wing—swept back. Circular tips.
Lower wing—straight. Aspect ratio=6.
Midspan stagger=0. G/c=1.0.
Decalage=0°. q=20.02 kg/m²
Reynolds No.=154,000.

$\alpha°$	C_D	C_L	$\alpha°$	C_D	C_L
−45	0. 657	−0. 538	15	0. 135	1. 095
−40	. 569	−. 549	16	. 148	1. 108
−35	. 482	−. 536	17	. 167	1. 091
−30	. 395	−. 508	18	. 205	1. 048
−27	. 340	−. 469	21	. 316	. 804
−24	. 285	−. 422	24	. 361	. 723
−21	. 242	−. 395	27	. 400	709
−18	. 206	−. 383	30	. 459	. 719
−15	. 170	−. 384	35	. 540	. 716
−14	. 154	−. 388	40	. 592	. 658
−13	. 137	−. 388	45	. 623	. 568
−12	. 119	−. 377	50	. 624	. 470
−9	. 038	−. 207	55	. 588	. 376
−6	. 024	−. 008	60	. 558	. 292
−3	. 023	+. 135	65	. 571	. 247
0	. 028	. 312	70	. 606	. 208
+3	. 040	. 500	75	. 636	. 161
6	. 057	. 673	80	. 655	. 093
9	. 079	. 892	85	. 669	+. 030
12	. 105	. 998	90	. 684	−. 032
14	. 123	1. 067			

TABLE XXIII

FORCE TEST

Clark Y biplane. 5-inch chord.
Upper wing—straight. Circular tips.
Lower wing—swept back. Aspect ratio=6.
Midspan stagger=0. G/c=1.0.
Decalage=0°. q=19.93 kg/m².
Reynolds No.=152,000.

$\alpha°$	C_D	C_L	$\alpha°$	C_D	C_L
−45	0. 510	−0. 434	15	0. 154	1. 141
−40	. 473	−. 476	16	. 168	1. 145
−35	. 413	−. 478	17	. 184	1. 133
−30	. 333	−. 433	18	. 201	1. 116
−27	. 287	−. 402	19	. 258	1. 041
−24	. 246	−. 372	21	. 343	. 908
−21	. 209	−. 347	24	. 435	. 816
−18	. 177	−. 341	27	. 496	. 813
−15	. 142	−. 354	30	. 554	. 810
−14	. 129	−. 359	35	. 654	. 799
−13	. 113	−. 358	40	. 742	. 770
−12	. 090	−. 327	45	. 804	. 738
−9	. 031	−. 146	50	. 864	. 667
−6	. 023	+. 004	55	. 913	. 589
−3	. 023	. 155	60	. 948	. 495
0	. 030	. 360	65	. 942	. 387
+3	. 043	. 552	70	. 886	. 275
6	. 069	. 735	75	. 816	. 176
9	. 089	. 905	80	. 727	. 088
12	. 118	1. 061	85	. 677	+. 022
13	. 128	1. 108	90	. 653	−. 036
14	. 140	1. 133			

TABLE XXIV

FORCE TEST

Clark Y biplane. 5-inch chord.
Upper wing—swept back. Circular tips.
Lower wing—straight. Aspect ratio=6.
Midspan stagger=+50 per cent chord $G/c=1.0$.
Decalage=0°. $q=20.00$ kg/m²
Reynolds No.=155,000.

$\alpha°$	C_D	C_L	$\alpha°$	C_D	C_L
−45	0.497	−0.377	15	0.143	1.162
−40	.486	−.448	16	.153	1.177
−35	.420	−.450	17	.168	1.171
−30	.337	−.406	18	.184	1.152
−27	.293	−.377	19	.239	1.046
−24	.250	−.349	21	.290	.952
−21	.215	−.328	24	.409	.873
−18	.181	−.317	27	.468	.820
−15	.150	−.335	30	.526	.825
−14	.138	−.343	35	.631	.831
−13	.123	−.355	40	.713	.796
−12	.104	−.345	45	.808	.741
−9	.037	−.192	50	.880	.680
−6	.024	−.033	55	.945	.608
−3	.023	+.150	60	.988	.515
0	.028	.343	65	.988	.411
+3	.040	.532	70	.951	.303
6	.060	.709	75	.896	.195
9	.084	.876	80	.837	.109
12	.111	1.042	85	.733	+.022
14	.133	1.135	90	.667	−.032

TABLE XXV

FORCE TEST

Clark Y biplane. 5-inch chord.
Upper wing—straight. Circular tips.
Lower wing—swept back. Aspect ratio=6.
Midspan stagger=−50% chord $G/c=1.0$.
Decalage=0°. $q=20.00$ kg/m²
Reynolds No.=154,000.

$\alpha°$	C_D	C_L	$\alpha°$	C_D	C_L
−45	0.629	−0.552	15	0.140	1.113
−40	.555	−.564	16	.155	1.124
−35	.473	−.554	17	.196	1.010
−30	.388	−.520	18	.233	.924
−27	.330	−.474	21	.332	.782
−24	.279	−.432	24	.379	.709
−21	.238	−.405	27	.428	.706
−18	.201	−.391	30	.498	.731
−15	.161	−.391	35	.600	.738
−14	.145	−.386	40	.614	.644
−13	.129	−.381	45	.583	.501
−12	.108	−.343	50	.569	.427
−9	.038	−.196	55	.571	.389
−6	.024	−.060	60	.576	.292
−3	.023	+.129	67.5	.576	.231
0	.028	.314	72.5	.612	.176
+3	.038	.507	77.5	.638	.118
6	.059	.700	82.5	.654	+.058
9	.083	.866	87.5	.670	−.007
12	.110	1.021	92.5	.729	−.072
14	.130	1.099			

TABLE XXVI

FORCE TEST

Biplane. 5-inch chord.
Upper wing—Clark Y. Circular tips.
Lower wing—N. A. C. A.-M1. Aspect ratio=6.
Stagger=0. G/c=1.0.
Decalage=0°. q=19.92 kg/m²
Reynolds No.=152,000.

$\alpha°$	C_D	C_L	$\alpha°$	C_D	C_L
−45	0.612	−0.579	15	0.168	0.917
−40	.560	−.625	16	.181	.914
−35	.481	−.634	17	.193	.899
−30	.388	−.593	18	.242	.847
−27	.330	−.559	21	.305	.734
−24	.284	−.529	24	.354	.714
−21	.244	−.509	27	.410	.727
−18	.207	−.522	30	.462	.744
−15	.169	−.522	35	.551	.738
−14	.151	−.518	40	.614	.700
−13	.134	−.506	45	.682	.639
−12	.112	−.488	50	.726	.558
−9	.050	−.339	55	.738	.488
−6	.027	−.163	60	.728	.393
−3	.020	−.017	65	.670	.294
0	.020	+.185	70	.593	.218
+3	.030	.371	75	.611	.178
6	.045	.539	80	.654	.119
9	.073	.715	85	.666	.059
12	.121	.880	90	.674	.004
14	.153	.914			

TABLE XXVII

FORCE TEST

Biplane. 5-inch chord.
Upper wing—N. A. C. A. M-1. Circular tips.
Lower wing—Clark Y. Aspect ratio=6.
Stagger=0. G/c=1.0.
Decalage=0°. q=19.99 kg/m²
Reynolds No.=154,000.

$\alpha°$	C_D	C_L	$\alpha°$	C_D	C_L
−45	0.581	−0.560	15	0.169	0.866
−40	.521	−.582	16	.182	.869
−35	.456	−.585	17	.196	.869
−30	.379	−.563	18	.210	.866
−27	.335	−.554	20	.264	.833
−24	.293	−.531	22	.324	.742
−21	.255	−.525	24	.369	.736
−18	.218	−.531	27	.412	.729
−15	.175	−.527	30	.465	.728
−14	.157	−.514	35	.534	.736
−13	.137	−.500	40	.630	.714
−12	.116	−.486	45	.699	.651
−9	.050	−.336	50	.734	.569
−6	.029	−.167	55	.756	.485
−3	.023	−.042	60	.750	.387
0	.023	+.150	65	.696	.281
+3	.031	.338	70	.609	.199
6	.049	.510	75	.608	.149
9	.075	.670	80	.644	.088
12	.127	.814	85	.652	+.025
14	.156	.858	90	.654	−.038

TABLE XXVIII

FLAT PLATES

Area ratio (a/A) and blocking correction (K) as determined from tests

$\alpha°$	3 by 18 inches		4 by 24 inches		5 by 30 inches		6 by 36 inches		7 by 42 inches	
	a/A	K	a/A	K	a/A	K	a/A	K	a/A	K
35°	0.0116	0.997	0.0179	0.989	0.0281	0.973	0.0392	0.953	0.0551	0.931
40°	.0121	.997	.0215	.990	.0336	.976	.0485	.950	.0658	.913
50°	.0144	.999	.0256	.996	.0405	.984	.0576	.946		
60°	.0163	.998	.0289	.996	.0453	.969	.0651	.911	.0888	.839
70°	.0177	.996	.0315	.988	.0492	.947	.0707	.880	.0962	.800
75°	.0181	.997	.0323	.990	.0505	.943	.0726	.871	.0988	.791
80°	.0187	.997	.0329	.988	.0515	.942	.0741	.870	.1008	.788
90°	.0188	.996	.0335	.987	.0522	.936	.0752	.860	.1023	.780

TABLE XXIX

FORCE TESTS—FLAT PLATES

C_L and C_D uncorrected for blocking.
C_L' and C_D' corrected for blocking.
Reynolds No.=153,000.
(For 3 by 18 inch plate q=55.20 kg/m²)
(For 4 by 24 inch plate q=31.05 kg/m²)
(For 5 by 30 inch plate q=20.00 kg/m²)
(For 6 by 36 inch plate q=13.79 kg/m²)

$\alpha°$	3 by 18 inch plate				4 by 24 inch plate			
	C_D	C_D'	C_L	C_L'	C_D	C_D'	C_L	C_L'
20°	0.366	0.366	0.976	0.976	0.340	0.340	0.933	0.931
25°	.444	.444	.872	.872	.432	.432	.886	.884
30°	.556	.556	.887	.886	.549	.549	.907	.905
35°	.689	.688	.939	.937	.691	.687	.944	.938
40°	.781	.780	.905	.903	.772	.767	.900	.894
45°	.859	.857	.816	.814	.839	.833	.816	.810
50°	.932	.930	.749	.747	.928	.918	.751	.743
55°	1.022	1.020	.676	.675	1.022	1.011	.691	.683
60°	1.110	1.108	.618	.617	1.111	1.097	.624	.616
65°	1.193	1.191	.543	.542	1.191	1.173	.546	.537
70°	1.260	1.256	.443	.441	1.270	1.249	.455	.447
75°	1.315	1.311	.355	.354	1.321	1.299	.356	.350
80°	1.361	1.357	.250	.249	1.374	1.350	.250	.246
85°	1.394	1.388	.136	.136	1.400	1.372	.135	.132
90°	1.399	1.390	.029	.029	1.413	1.385	.028	.027
	5 by 30 inch plate				6 by 36 inch plate			
20°	0.342	0.341	0.957	0.954	0.344	0.341	0.950	0.940
25°	.426	.423	.867	.861	.436	.428	.903	.887
30°	.546	.540	.925	.915	.581	.566	.992	.966
35°	.723	.713	.952	.937	.719	.693	1.014	.978
40°	.794	.778	.932	.914	.811	.772	.958	.912
45°	.861	.841	.839	.819	.904	.848	.890	.835
50°	.942	.913	.789	.765	.995	.921	.841	.779
55°	1.042	1.006	.740	.714	1.100	1.006	.796	.728
60°	1.160	1.113	.670	.643	1.215	1.095	.721	.650
65°	1.244	1.188	.577	.551	1.322	1.178	.640	.570
70°	1.315	1.250	.484	.460	1.428	1.257	.939	.474
75°	1.405	1.331	.386	.366	1.501	1.310	.427	.372
80°	1.441	1.361	.269	.254	1.572	1.363	.304	.262
85°	1.473	1.389	.145	.137	1.614	1.392	.174	.150
90°	1.488	1.400	.026	.024	1.613	1.400	.044	.038

TABLE XXIX—Continued

FORCE TESTS—FLAT PLATES

C_L and C_D uncorrected for blocking.
Reynolds No.=153,000.
(For 7 by 42 inch plate q=10.17 kg/m²)

$\alpha°$	7 by 42 inch plate		$\alpha°$	7 by 42 inch plate	
	C_D	C_L		C_D	C_L
20°	0. 338	0. 982	60°	1. 318	0. 775
25°	. 420	. 914	65°	1. 445	. 689
30°	. 584	. 989	70°	1. 567	. 579
35°	. 727	1. 036	75°	1. 650	. 467
40°	. 843	1. 000	80°	1. 716	. 339
45°	. 926	. 921	85°	1. 761	. 198
50°	1. 042	. 888	90°	1. 777	. 055
55°	1. 195	. 848			

TABLE XXX

FORCE TESTS—CLARK Y WINGS

Aspect ratio=8. Circular tips.
C_L and C_D uncorrected for blocking.
C_L' and C_D' corrected for blocking.
Reynolds No.=153,000.

(For 3-inch chord q=55.10 kg/m²) (For 5-inch chord q=20.05 kg/m²)

$\alpha°$	3-inch chord				$\alpha°$	5-inch chord			
	C_D	C_D'	C_L	C_L'		C_D	C_D'	C_L	C_L'
26°	0. 479	0. 479	0. 868	0. 868	27. 75°	0. 528	0. 519	0. 914	0. 898
28°	. 527	. 527	. 908	. 907	29. 70°	. 578	. 567	. 946	. 928
30°	. 572	. 571	. 932	. 930	32. 70°	. 654	. 638	. 968	. 945
35°	. 701	. 700	. 954	. 952	35. 70°	. 742	. 721	. 980	. 952
40°	. 807	. 805	. 915	. 912	37. 70°	. 795	. 769	. 965	. 934
45°	. 888	. 885	. 843	. 840	39. 75°	. 838	. 808	. 959	. 925
50°	. 942	. 939	. 752	. 750	44. 85°	. 916	. 876	. 906	. 866
55°	1. 005	1. 002	. 675	. 675	50. 00°	. 986	. 934	. 800	. 757
60°	1. 084	1. 080	. 602	. 599	55. 15°	1. 081	1. 015	. 723	. 676
65°	1. 146	1. 139	. 519	. 515	60. 25°	1. 180	1. 095	. 646	. 599
70°	1. 210	1. 202	. 430	. 427	65. 45°	1. 260	1. 160	. 560	. 515
75°	1. 266	1. 258	. 326	. 324	70. 65°	1. 348	1. 230	. 453	. 413
80°	1. 300	1. 290	. 226	. 224	75. 85°	1. 400	1. 270	. 344	. 312
85°	1. 314	1. 305	. 123	. 122	81. 05°	1. 446	1. 304	. 216	. 195
90°	1. 322	1. 312	. 013	. 013	86. 25°	1. 470	1. 322	. 089	. 080
					91. 50°	1. 465	1. 317	—. 043	—. 039

Langley Memorial Aeronautical Laboratory,
National Advisory Committee for Aeronautics,
Langley Field, Va., *July 31, 1928.*